GEAP-4158

SODIUM COOLED REACTORS PROGRAM

Fast Ceramic Reactor Development Program

Fifth Quarterly Report, October – December 1962

Edited by
F. J. Leitz

January 1963

Atomic Power Equipment Department
General Electric Company
San Jose, California

UNITED STATES ATOMIC ENERGY COMMISSION • DIVISION OF TECHNICAL INFORMATION

LEGAL NOTICE

Printed in USA. Price $1.75. Available from the Office of Technical Services, Department of Commerce, Washington 25, D. C.

USAEC Division of Technical Information Extension, Oak Ridge, Tennessee

GEAP-4158
REACTOR TECHNOLOGY

SODIUM-COOLED REACTORS PROGRAM

FAST CERAMIC REACTOR DEVELOPMENT PROGRAM

Fifth Quarterly Report

October-December, 1962

Prepared for the
United States Atomic Energy Commission
Under
Contract No. AT(04-3)-189, Project Agreement No. 10

January 1963

ATOMIC POWER EQUIPMENT DEPARTMENT
GENERAL ELECTRIC
SAN JOSE, CALIFORNIA

TABLE OF CONTENTS

TABLE OF CONTENTS (Continued)

LIST OF ILLUSTRATIONS

SECTION I

INTRODUCTION

The Fast Ceramic Reactor Development Program is an integrated analytical and experimental program directed toward the development of fast reactors employing ceramic fuels, with particular attention to mixed plutonium-uranium oxide. Its major objectives are:

a. Development of a reliable, high performance fast reactor having nuclear characteristics which provide stable and safe operation, and

b. Demonstration of low fuel cycle cost capability for such a reactor, primarily through achieving high burnup of ceramic fuels operating at high specific power.

Progress during the period October 1 - December 31. 1962 on the currently active tasks of this program is described in subsequent sections.

This is the fifth in a series of quarterly progress reports written in partial fulfillment of Contract AT(04-3)-189, Project Agreement No. 10, between the United States Atomic Energy Commission and the General Electric Company. Prior progress reports to the Commission under this contract include the following:

Monthly Progress Letters, Nos. 1-39, from July 1959 through November 1962.

GEAP-3888 FCR Development Program - First Quarterly Report; October - December, 1961.

GEAP-3957 FCR Development Program - Second Quarterly Report, January-March, 1962.

GEAP-3981 FCR Development Program - Third Quarterly Report, April - June, 1962.

GEAP-4080 FCR Development Program - Fourth Quarterly Report, July - September, 1962.

In addition, the following topical reports have been issued:

GEAP-3287 Fast Oxide Breeder - Reactor Physics, Part I - Parametric Study of 300 MWe Reactor Core. P. Greebler, P. Aline, J. Sueoka; November 10, 1959.

GEAP-3347 Fast Oxide Breeder - Stress Considerations in Fuel Rod Design. K. M. Horst; March 28, 1960.

GEAP-3486 Fast Oxide Breeder Project - Fuel Fabrication.

Part I - Plutonium-Uranium Dioxide Preparation and Pelletized Fuel Fabrication. J. M. Cleveland, W. C. Cavanaugh;

Part II- Fabrication of Plutonium-Uranium Dioxide Specimens by Swaging. M. E. Snyder, W. C. Cowden, August 15, 1960.

GEAP-3487 Fast Oxide Breeder - Preliminary Sintering Studies of Plutonium-Uranium Dioxide Pellets. J. M. Cleveland, W. C. Cavanaugh; August 15, 1960.

GEAP-3636 Calculation of Doppler Coefficient and Other Safety Parameters for a Large Fast Oxide Reactor. P. Greebler, B. A. Hutchins, J. R. Sueoka; March 9, 1961.

GEAP-3721 Core Design Study for a 500 MWe Fast Oxide Reactor. K. M. Horst, B. A. Hutchins, F. J. Leitz, B. Wolfe; December 28, 1961.

GEAP-3824 Fabrication Cost Estimate for UO_2 and Mixed PuO_2-UO_2 Fuel. G. D. Collins; January 24, 1962.

GEAP-3833 The Post-Irradiation Examination of a PuO_2-UO_2 Fast Reactor Fuel. J. M. Gerhart; November 1961.

GEAP-3856 Experimental Fast Oxide Reactor. K. P. Cohen, M. J. McNelly, B. Wolfe; November 27, 1961.

GEAP-3876 Plutonium Fuel Processing and Fabrication for Fast Ceramic Reactors. H. W. Alter, G. D. Collins, E. L. Zebroski; February 1, 1962.

GEAP-3880 Comparative Study of PuC-UC and PuO_2-UO_2 as Fast Reactor Fuel. Part I - Technical Considerations. K. M. Horst, B. A. Hutchins; February 15, 1962.

GEAP-3885 Experimental Fast Ceramic Reactor Design. Status Report as of October 31, 1961. Edited by K. M. Horst; April 24, 1962.

GEAP-3923 Resonance Integral Calculations for Evaluation of Doppler Coefficients - The RAPTURE Code. J. H. Ferziger, P. Greebler, M. D. Kelley, J. Walton; June 12, 1962.

GEAP-4028 A Fuel Reprocessing Plant for Fast Ceramic Reactors. H. W. Alter; February 1, 1962.

GEAP-4058 Analytical Studies of Transient Effects in Fast Reactor Fuels. R. B. Osborn and D. B. Sherer; August, 1962.

GEAP-4090* FORE - A Computational Program for the Analysis of Fast Reactor Excursions. P. Greebler, D. B. Sherer; October, 1962.

GEAP-4130* Experimental Studies of Transient Effects in Fast Reactor Fuels, Series I, UO_2 Irradiations. J. H. Field; November 15, 1962.

*AEC approval of general distribution pending.

SECTION II

SUMMARY

2.1 Task B - Vented Fuel Development

The first series of six sodium logging experiments was successfully completed utilizing UO_2 fuel pins. No changes in defected fuel clad dimensions were observed after cycling pin linear power from 0 to 20-26 kw/ft, nor was any damage observed on cycling (to 22 kw-ft) of a non-defected specimen which had been fabricated to contain sodium in its cored center. A second series of three capsules utilizing mixed PuO_2-UO_2 fuel has been designed and the capsule components fabricated. Meltable and dissolvable plugs of soft solder and silver solder have been developed to permit fabrication of plutonium-bearing fuel specimens in existing equipment.

In continuing sodium-UO_2 and sodium-mixed oxide compatibility tests, disintegration of certain low density UO_2 pellets in stagnant sodium at 1000 F has been observed.

Conceptual design of an in-pile capsule experiment to determine release of fission products from mixed oxide fuel into sodium coolant has been completed. Design of an experiment to study fission product plugging in a long fuel specimen is underway.

Preliminary design and cost estimation of in-pile sodium loops and loopsules has been completed. Loopsules in the GETR are recommended as the most economical and technically feasible procedure for conducting experiments planned for the investigation of fission product release to and distribution in flowing sodium coolant.

2.2 Task C - Fuel Testing in TREAT

Series I testing has been completed and a topical report (GEAP-4130) discussing the results has been written. Five tests were conducted in this series (1 inch diameter UO_2 fuel) and incipient failure limits identified for single and repeated transients. Approval has been received from TREAT management for the initial Series II (0.25 inch diameter PuO_2-UO_2 fuel) irradiation

and the first capsule has been sent to the TREAT site. Pre-irradiation of Series III (0.25 inch diameter, pre-irradiated PuO_2-UO_2 fuel) pins is ready to begin if conducted in GETR, but awaits a decision on which test reactor will be used (GETR or MTR-ETR).

2.3 Task D - Mixed Carbide Fuel Study

Topical report, GEAP-3880. Comparative Study of PuC-UC and PuO_2-UO_2 as a Fast Reactor Fuel. Part II - Economic Considerations, has been written and issued. Estimated fuel cycle costs for two carbide reactor and fuel designs are compared with that previously estimated for a reference oxide design. A limited cost saving potential for carbide fuel relative to oxide fuel (0.16 mill/kwh on a 1975 basis) is indicated provided fuel and clad ratings are achieved which are beyond the reach of present technology. This margin is insufficient to warrant a change in direction of development from the relatively well matured oxide technology for the first developmental FCR plants.

2.4 Task E - Fuel Performance Evaluation

Development of methods to measure fuel temperature in-pile is in progress, using temperature sensing elements for short-term, and gas thermometry for long-term irradiations. Improvements in control of fuel composition and uniformity of irradiation conditions are under investigation for application to irradiation tests of fuel to high burnup. Experiments are being planned to establish whether plutonium migrates under isothermal conditions as a function of axial gradients in either uranium-plutonium composition or plutonium isotopic composition (self-diffusion).

Sintering of plutonium oxide under current "reference" conditions has been shown to give an O/Pu ratio of 1.852 ±0.003, in good agreement with thermodynamic prediction. From this result and the previously observed 2.006 O/U ratio for uranium oxide, an O/U + Pu ratio of 1.975 is calculated for 20% Pu-80% U mixed oxide, assuming simple pro rata contributions to mixed oxide stoichiometry from the separate oxides.

2.5 Task G - Reactor Dynamics and Design

Several modifications of FCR core design and operating conditions are being evaluated

on the basis of new cross section data and improved calculation methods, aiming at a best balance between safety parameters and fuel economics.

A 17 per cent increase in Doppler coefficient is indicated to correct earlier reference FCR values calculated on an isothermal basis for the spatial flux and temperature distribution in the core and individual fuel rods. Over the range of expected Debye temperature for mixed oxide, crystalline binding in the oxide lattice is calculated to have only a small effect on the Doppler coefficient.

Reports have been written on the FORE computer code for analysis of reactor transients (GEAP-4090) and on Doppler calculation methods (GEAP-4092). Drafts have been prepared of reports on the results of calculations using the FORE code and on the FARM code for analysis of fast reactor meltdown accidents.

SECTION III

TASK B - VENTED FUEL DEVELOPMENT

3.1 Sodium Logging

3.1.1 Series I - UO_2 Fuel

3.1.1.1 Specimen B-1-E

The sixth and final capsule of the first series of defected fuel specimens, B-1-E, was irradiated for eight thermal cycles in which its linear power generation was varied from 0 kw/ft to 26 kw/ft ±15 per cent. Figure 3-1 shows the sodium-temperature versus time history of the irradiation. From the observed range of sodium temperature during the power cycle, 1030 F to 1150 F, the specimen clad outer surface temperature is calculated to have been 1140 F to 1240 F. Calculation of the in-pile linear rod power is based upon the measured temperature drop across the annular thermal barriers and the available calorimetric data.

As with the previous capsules which had been irradiated at lower rod power, no clad distortion occurred on power cycling, as evidenced by the agreement between pre- and post-irradiation measurements of the specimen diameter. Figure 3-2 shows transverse cross sections of specimen B-1-E made at 1.1 inches and 2.1 inches from the bottom of the fuel pin (overall length 3.3 inches). These photographs confirm visual examination which indicated that sodium readily entered the cracks and gaps in the fuel pellet and the fuel-clad gap.

3.1.1.2 Comparison of Defected Specimens

Surfaces from specimens B-1-A, B-1-B, B-1-C, B-1-D, and B-1-E, were rough polished as part of the post-irradiation examination. Figure 3-3 shows the five surfaces for comparison; design and operating conditions for these five capsules, as well as for B-1-F, are given in Table III-1. All fuel pins were loaded with five half-inch-long sintered pellets of

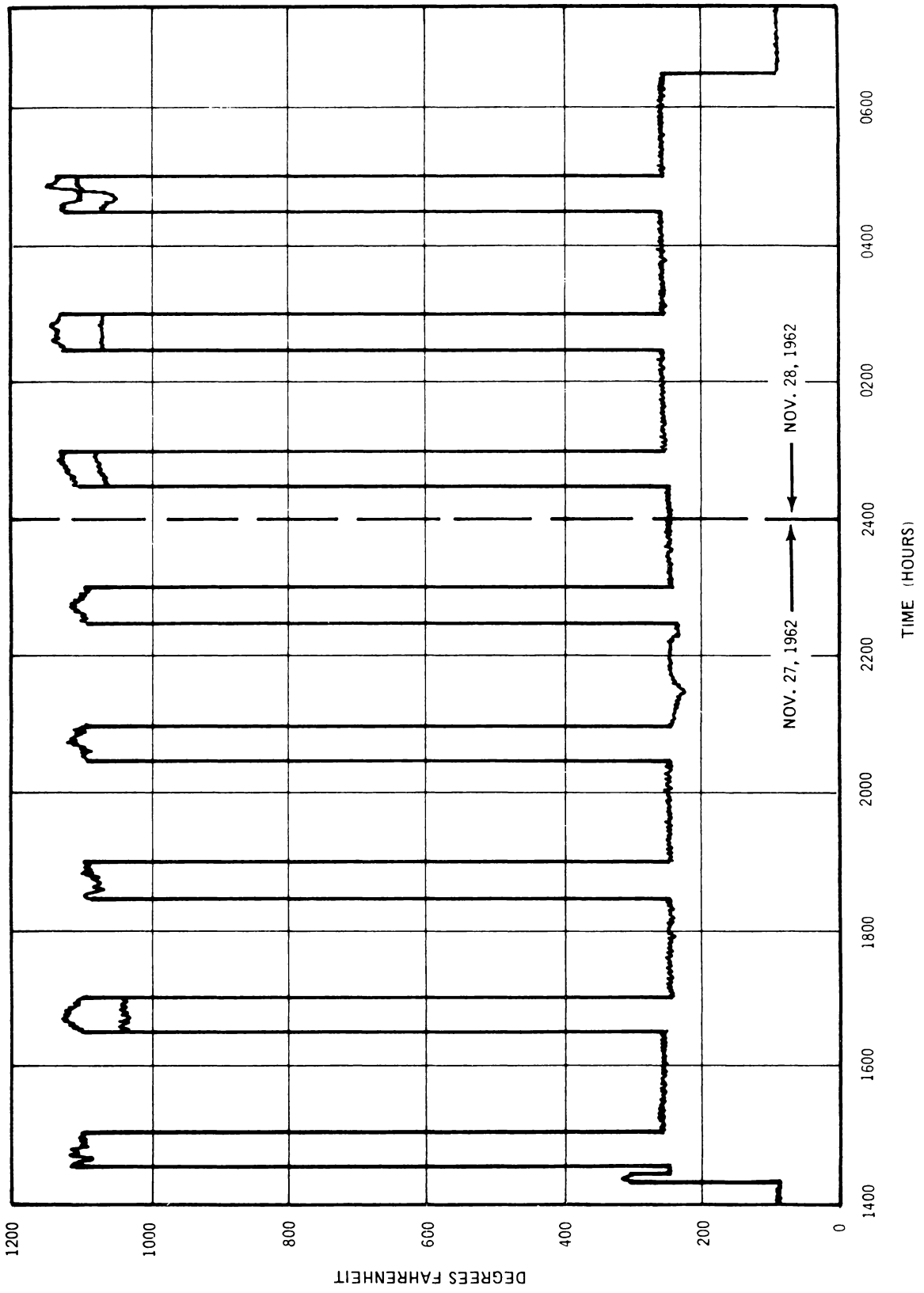

FIGURE 3-1 CAPSULE B-1-E SODIUM TEMPERATURE VS. TIME

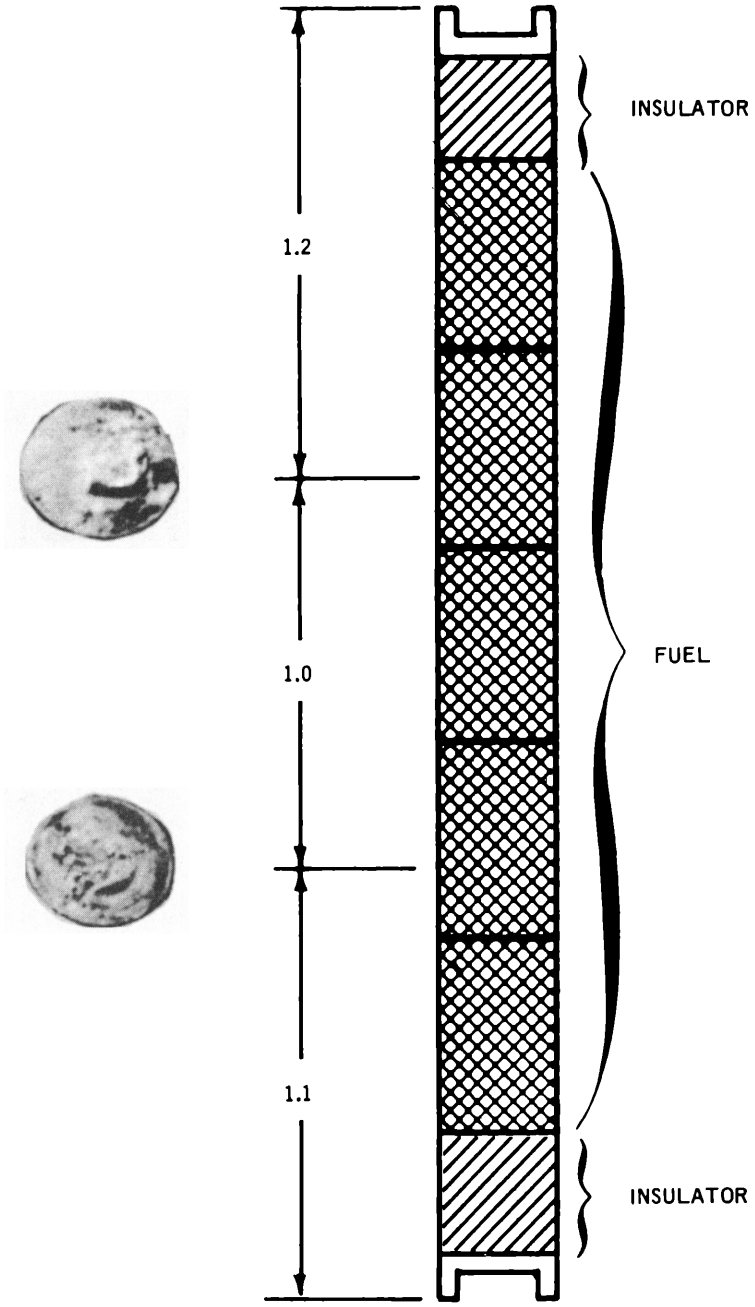

FIGURE 3-2 SPECIMEN B-1-E, TRANSVERSE CROSS SECTIONS OF FUEL SPECIMEN

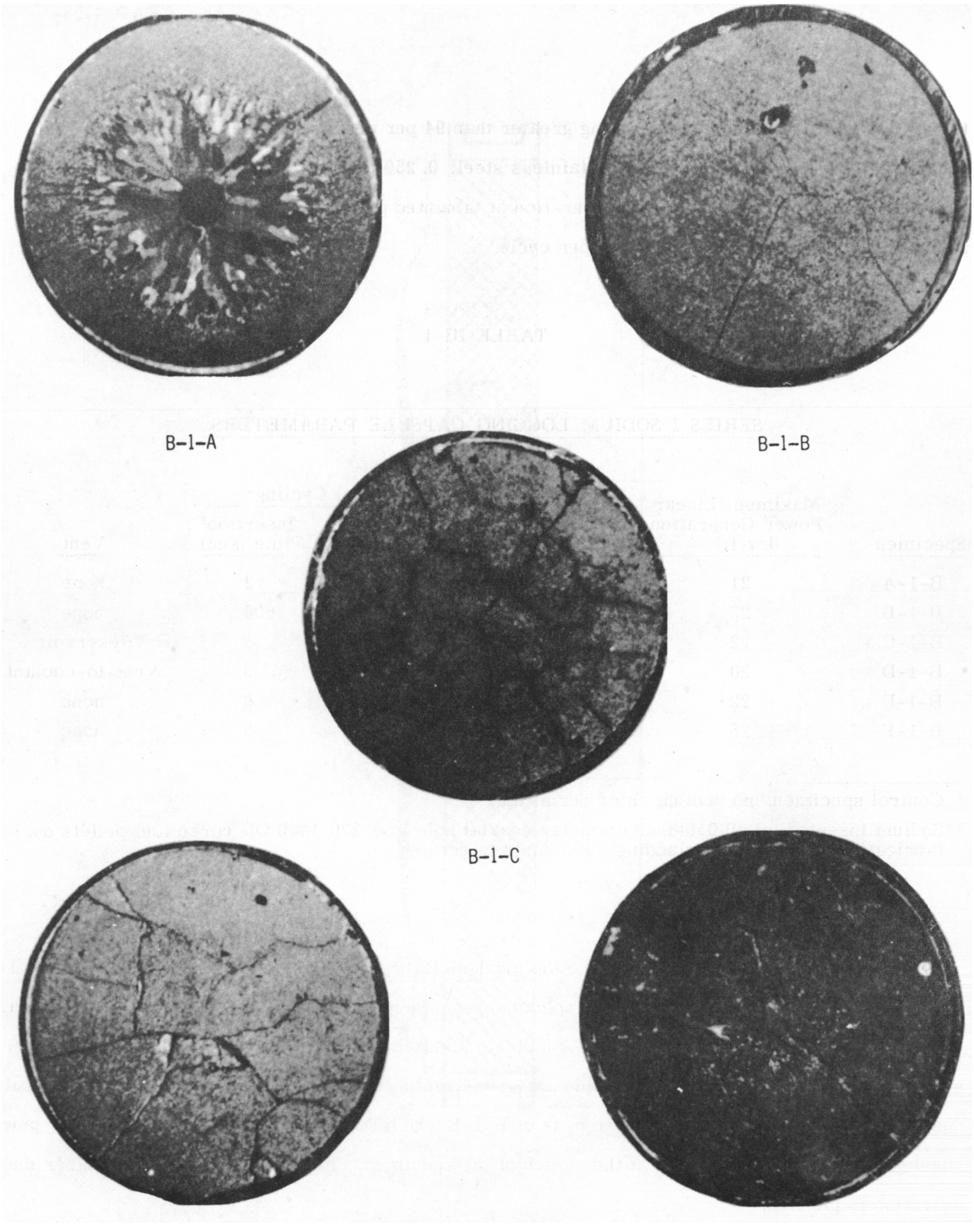

FIGURE 3-3 ROUGH POLISH CROSS SECTIONS OF SODIUM LOGGING SPECIMENS

UO_2, 19.3 per cent enriched and having greater than 94 per cent theoretical density and an O U ratio of 2.006. The cladding was 304 stainless steel, 0.250 inch OD × 0.006 inch wall thickness. Thermal cycling consisted of in-pile operation at tabulated power for thirty minutes per cycle, followed by logging for ninety minutes per cycle.

TABLE III-1

SERIES I SODIUM LOGGING CAPSULE PARAMETERS

Specimen	Maximum Linear Power Generation (kw/ft)	Defect Diameter (inches)	Thermal Cycling		Vent
			Number of Cycles	Insertion Time (sec)	
B-1-A	21	none*	5	3	none
B-1-B	23	0.005	7	600	none
B-1-C	22	0.005	7	3	Reservoir
B-1-D	20	0.005	8	3	Vent-to-coolant
B-1-E	22	0.005	8	3	none
B-1-F	26	none**	1	3	none

* Control specimen, no sodium entry permitted.

**Sodium inserted into 0.050-inch diameter coaxial hole in 0.220-inch OD cored fuel pellets during fabrication. No defect in cladding for sodium to escape.

In Figure 3-3, note the marked difference between the control specimen B-1-A, which had no defect, and the four other specimens which operated with defects. The large central void and extensive grain growth in B-1-A indicate high temperature operation. In the other specimens, the absence of large central voids and gross grain growth suggest cooler operation, probably due to the presence of sodium. In the case of B-1-E which was operated at the highest linear power, some grain growth is evidenced at the center of the specimen. Further examination at higher magnification is planned.

3.1.1.3 Specimen B-1-F

Specimen B-1-F was designed to simulate a hypothetical "worst" case, where sodium had seeped into the axial void without filling the pellet-to-clad gap and where the defect had become plugged so as to prevent pressure relief. The specimen contained one solid pellet and four cored pellets with sodium filling the coaxial hole.

Previously, transverse sectioning had revealed that only one of eight sections contained sodium in the central void. In the unpolished condition it was not possible to detect any radial distribution of the sodium within these sections.

Longitudinal sections were therefore made and polished to establish whether axial redistribution of fuel and sodium had occurred. Figure 3-4 shows one section made from the piece that contained both the cored and uncored pellets. Although gross axial redistribution was not found, the polished and X10 magnified views of these specimens revealed that the sodium had distributed radially. Based upon RML experience in viewing sodium-soaked uranium oxide pellets, the white phase seen in the fuel-clad gap, in the cracks in both the cored and uncored pellets, and in the central void is identified as sodium oxide. Thus, the sodium evidently migrated from the central void through cracks in the fuel to a cooler region where it deposited.

The distribution of sodium within the fuel and gaps evidently has a pronounced effect on fuel operating temperatures. No clad deformation was noted in specimen B-1-F even though the calculated yield pressure is equivalent to the sodium vapor pressure at a temperature of only 3000 F.

The grain structure in the uncored pellet shown in Figure 3-4 is further evidence of cooler fuel operation caused by the presence of sodium. Grain growth is apparent but not to the same degree as the control sample.

3.1.2 Series II

Capsule components have been fabricated for the second series of three capsules which contain mixed PuO_2-UO_2 fuel specimens.

FIGURE 3–4 LONGITUDINAL SECTION OF SPECIMEN B–1–F

A method has been developed to size precisely the inside diameter of cladding for Series II fuel, so that close "as-fabricated" fuel-clad gaps can be maintained. The fuel-clad gap is considered a key variable in this series of tests, especially for the specimen with sodium fabricated into the cored fuel, since it is desired to preclude sodium from flowing from the fabricated central void into any larger void volume at a substantially lower temperature. The condition of minimum fuel-clad gap axially and radially is intended to represent the normally observed case where irradiated fuel pellets have expanded radially and closed the pellet-to-clad gap.

The fuel clad inner diameter is sized with a "ballizing" technique. In this technique a precision diameter tungsten carbide ball (0.2203 inch) is forced through a slightly undersized (0.218-inch ID) piece of cladding. The expanded cladding has a finished ID of 0.220-inch to 0.221-inch. Use of this cladding and selected pellets permits control of the fuel-clad gap to less than 0.003-inch on the diameter.

Fuel specimen B-2-A was successfully fabricated and helium leak-checked, and is now being measured prior to assembly into the test capsule.

Fuel pellets for specimen B-2-B were drilled with 0.049 - 0.054-inch axial holes and the holes were filled with sodium. The fuel specimen was then assembled and helium leak-checked. A leak was found and the end cap was rewelded in an effort to seal the leak. The fuel specimen is presently being rechecked for leaks.

A silver solder defect plug has been developed and is being proof-tested on a dummy specimen for use on specimen B-2-C. The solder composition is 56 per cent silver, 22 per cent copper, 17 per cent zinc, and 5 per cent tin. The melting point is 1145 F and the flow point is 1205 F.

The plug was initially tested by placing a dummy pin with a 0.005-inch diameter plugged defect into sodium and raising the sodium temperature in 50 F increments from a starting temperature of 260 F. After each temperature increase, the temperature was held constant for about thirty minutes. The plug opened a clean, smooth hole at 1050 F after a total elapsed time from 260 F of seven and three-quarter hours. Since the plug opened below its melting point, it is

assumed that the plug removal mechanism is dissolution. However, it is evident from the foregoing test that the capsule may be successfully filled with sodium at low temperature ($\leq$ 280 F) without opening the defect.

An end cap was successfully welded onto a dummy pin containing a silver solder defect plug, thus showing that welding heat does not destroy a plug located one and a half inches away from the end cap. This welding was performed in the actual loading and welding facility to be used for Specimen B-2-C.

3.2 Sodium-Fuel Compatibility

3.2.1 UO_2

The FCR sodium loop in Building D has been modified to improve operation and control. The loop has been seasoned through about 1800 hours of testing operation at 700 F to 1000 F. The minimum steady-state oxygen concentration levels possible at 700 F through 1000 F are currently being determined.

The preparation, characterization, and analysis of non-stiochiometric UO_2 pellets has continued in order to prepare test fuel for the sodium loop. The procedures developed have not been successful in producing high density annular pellets to date. The first procedure employed was to cold press mixtures of UO_2 and U_3O_8, then sinter in molybdenum boats at 1450 C in an atmosphere of wet hydrogen. Control of the O/U ratio was attempted by varying the soaking time at 1450 C. Pellets produced in this manner gave average O/U ratios near 2.02 (the desired range of O/U ratio was 2.01 to 2.2) and all were only 70 to 85 per cent of theoretical density. Further investigation revealed that the O/U ratio varied considerably within the pellets, with a typical surface value of 2.044 and mid-radius value of 2.013.

A second procedure was tried in which cold pressed mixtures of UO_2 and U_3O_8 were sintered in argon at 1450 C. Pellets with O/U ratio of 2.185 were produced in this manner but the density was again low at 85 per cent of theoretical. A leak in the argon gas system was detected subsequent to sintering these pellets so that the results are suspect. A second attempt to produce high density

pellets will be made as soon as the furnace is repaired. Both uniformly oxidized powders and mixtures of UO_2 and U_3O_8 will be sintered in subsequent tests.

A series of scouting tests has been completed using a heated pot of sodium and the fuel pellets described above in addition to high density UO_2 pellets produced by the standard sintering technique in hydrogen at 1600 C. These tests were considered as a precursor to loop tests where oxygen concentration in the sodium will be known and controlled. In these pot tests, all low density pellets disintegrated when heated to 1000 F in sodium for one to seven hours over the entire range of O/U composition from 2.06 down to 2.005. On the other hand, pellets sintered by the standard reduction technique, with O/U ratio of 2.009, suffered no change under identical treatment. Thus, the density and porosity of the pellets or some other phenomenon evidently affects their reaction with sodium. Apparent solid density and bulk density measurements on one low density pellet (80 per cent theoretical) indicate an open porosity of about 18 per cent and a closed porosity of about 2 per cent of the compact volume.

Further tests are planned as soon as appropriate pellets can be produced in the argon sintering furnace.

3.2.2 Mixed Oxide

Nine capsules for sodium-mixed oxide compatibility tests have been fabricated - four for testing of previously irradiated fuel, the remainder for unirradiated fuel testing. The capsules have been filled with sodium and selected fuel pellets, covered with argon, and welded closed. Testing, for a twenty hour period each, is in progress. Single unirradiated pellets with compositions 0, 20, 28, and 100 per cent PuO_2 (with UO_2) are included. In addition, one 20 per cent PuO_2 pellet was heated in air at 750 C for one hour in an attempt to make a pellet with greater than stiochiometric oxygen content. Irradiated oxide selected for study consists of samples from specimens irradiated during Phase I of the FCR program, including both pelleted and swaged, high burnup fuel.

3.3 Fission Product Plugging

3.3.1 Specimen IX-1-P

Six additional longitudinal samples from specimen IX-1-P were selected and analyzed radiochemically for strontium-90, zirconium-95, cerium-144, cesium-134, and cesium-137, to further define the axial variation in fission product concentration. The new analyses are shown in Figure 3-5 along with the data previously reported (GEAP-3957, FCR Second Quarterly Report) using nine similar samples. Comparison of the new data to those given in GEAP-3957, Figure IV-2, shows a better definition of both ends of the fission product distribution curve. It also shows that there is a real peaking of fission products in the pellet interface regions.

As indicated previously, there was no appreciable transport of zirconium and cerium across the fuel-insulator region. Less strontium migrated than was previously noted; slight concentrations of strontium appear in interface regions. Gross transport of cesium-134 is indicated (cesium-134 is formed from an (n,γ) reaction with cesium-133), and considerable cesium-137 (directly formed in fission) also migrates out of the fuel region.

Isotherms were calculated for the fuel-blanket interface region of the specimen in an attempt to understand the pronounced peaking of cesium-137 and cesium-134 on the fuel side of the interface. Figure 3-6 shows the calculated isotherms and the corresponding region in IX-1-P. A central void was observed in the specimen consistent with the isotherm map. However, the Figure 3-6 photograph does not show the void because the photographed surface is below the center line of the specimen.

Comparing the isotherms from Figure 3-6 with the axial fission product distribution shown in Figure 3-5, it appears as though the same axial portion of the specimen contained both the highest fuel temperatures and the highest concentrations of fission products. This does not necessarily mean that the peak fission product concentrations and peak temperatures occurred at the same point radially. Radial samples from specimens V-1-S and V-2-P show that volatile fission products, especially cesium, migrate away from the hot center of the fuel to the cooler periphery.

Proportionately more cesium was found in sample 58 than other fission products despite the fact that most of the fuel in this sample was above 3500 F and that cesium has been shown to migrate away from hot fuel regions. Thus, it is tentatively concluded that cesium concentrated in the peripheral void region of this sample. It is hypothesized that part of the cesium generated in the fuel might vaporize and be swept toward the gas reservoir. The first cool volume encountered enroute would be the peripheral void between the fuel and insulator pellets where it would tend to condense and concentrate, thus raising the cesium content of that region.

3.3.2 Fission Product Plugging Capsules

Investigations of specimens IX-1-P, V-1-S, and V-2-P have indicated that certain fission products tend to concentrate on the surfaces of oxide fuel and blanket pellets and in the pellet-pellet and pellet-clad gaps. Since such performance may be detrimental to the performance of FCR fuel when large amounts of fission products are generated, it is proposed to investigate long fuel rods irradiated to high burnups. Such rods would generate gaseous and volatile fission products and force them to flow through cooler regions of fuel and blanket before reaching the reservoir or a vent.

The experiment will consist of two capsules, each containing one fuel rod irradiated to a maximum burnup of ~100,000 MWD/T. One specimen will simulate the hottest FCR fuel rod, including the sharp change in central temperatures and rod power associated with the fuel-blanket interface. The second specimen is intended to be representative of lower power rods by having part of its active fuel zone extend beyond the top of the test reactor core. This will permit the specimen power density to drop off to a low value before reaching the fuel-blanket interface. In-pile pressure monitoring of both specimens will show the degree of communication between the end of the fuel pin and the gaseous fission products released to the fuel. The designs feature an overall length of 51 inches with 27 inches of mixed oxide fuel and 15 inches of natural UO_2 blanket in the high power rod, and 40 inches of fuel and 5 inches of blanket in the low power rod. Peak $\int k d\theta$ of 5500 Btu/hr-ft and burnup to 100,000 MWD/T are the planned operating conditions. The power at the fuel-blanket interface is targeted for 50 per cent of the peak power to simulate the FCR axial power profile. Post-irradiation examination of the specimens will include measurement of axial and radial distribution of fission products in the fuel and blanket regions, dimensional changes, and fission gas release.

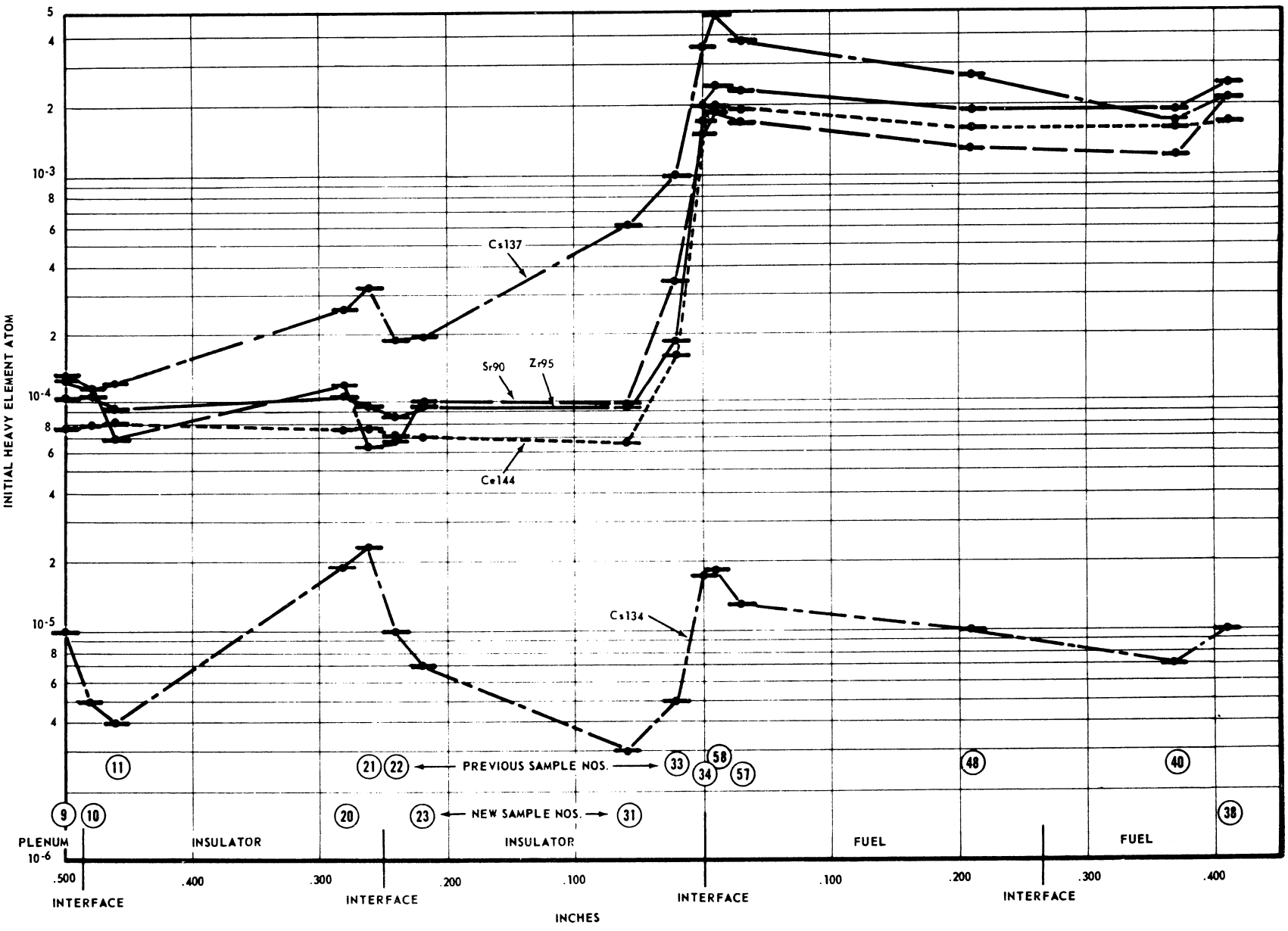

FIGURE 3–5 AXIAL FISSION PRODUCT DISTRIBIITION IN SPECIMEN IX–1–P

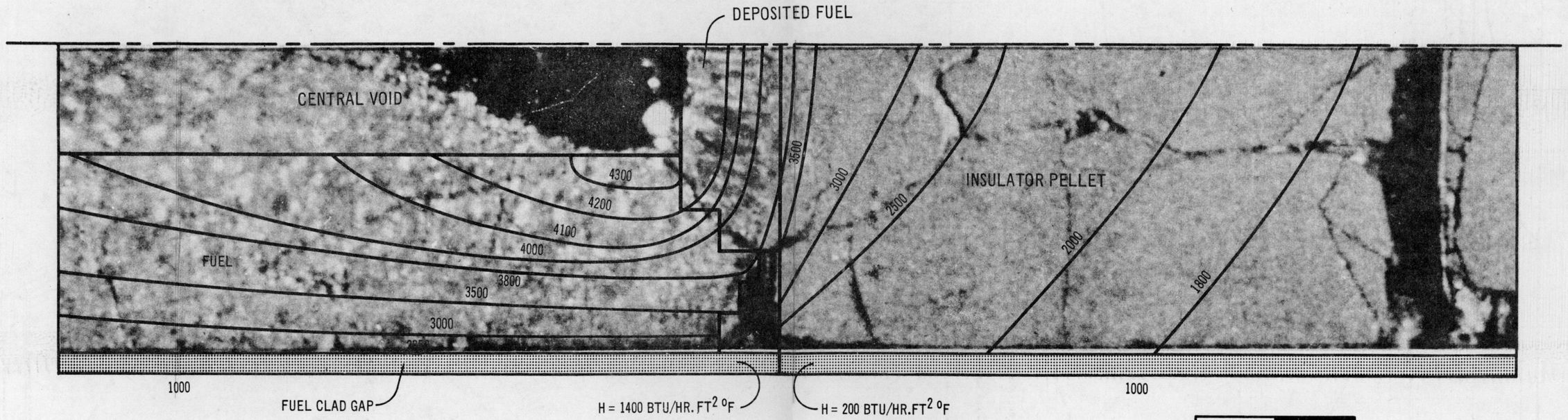

FIGURE 3-6 CALCULATED ISOTHERMS IN SPECIMEN IX-1-P

3.4 Fission Product Release

Conceptual design has been completed and detailed design has started on a capsule experiment to study release of fission products from mixed oxide fuel into static sodium. The concept features three doubly encapsulated fuel specimens in a single capsule. The specimens will be designed to simulate (1) vented fuel without a blanket, (2) fuel vented through a natural UO_2 blanket, and (3) fuel vented through a defect. Two specimens will be designed to operate at peak $\int k d\theta$ of 5000 Btu/hr-ft while the third will operate at 4000 Btu/hr-ft.

Post-irradiation examination will include radiochemical analysis of the sodium and cover gas to identify the fission products which escape oxide fuel operated near FCR reference conditions and those retained by the sodium. These data will be valuable for predicting shielding requirements and maintenance problems in both sodium reactor and sodium loop applications wherein oxide fuels are used.

3.4.1 Loop-Loopsule Study

Disposable sodium loopsules have been compared with a standard sodium loop for testing the system effects caused by intentionally and inadvertently vented (defected) fuel. Both economic and technical considerations favor the loopsule approach.

Existing thermal reactor facilities have been reviewed as possible test beds, on the basis of which the GETR pool is recommended as the most economical as well as the most technically feasible location for installation of loopsules.

During the report period, a loop was conceived and designed to a point permitting preliminary cost estimation. In addition, the loopsule previously reported has been modified to be a more compact unit. Cost estimation of both installations has been completed.

A memorandum report has been prepared which describes the two designs and evaluates the technical and economic aspects of a five year test program for each.

SECTION IV

TASK C - FUEL TESTING IN TREAT

4.1 Series I Tests

Irradiation and examination of five EFCR-type pins (1 inch diameter, segmented UO_2 fuel) has been completed (see prior quarterly reports, GEAP-3957, January-March; GEAP-3961, April-June; and GEAP-4080, July-September, 1962). The severity of transients (single and repeated) necessary to cause damage has been identified and the adequacy of the proposed EFCR design concept is being evaluated. Post-irradiation examination has indicated several areas for subsequent investigation, and the fuel will be kept in accessible storage pending further need for information.

A topical report (GEAP-4130) discussing transient studies of fast reactor fuels has been written and will be issued shortly. Portions of this report including conclusions from the irradiation, examination, and analysis of the Series I fuel specimens, are summarized in the following paragraphs.

4.1.1 Postulated Sequence of Events in a Power Transient

On the basis of the results of post-irradiation examinations, a sequence of events associated with severe power transients in SS clad UO_2 fuel may be postulated, to serve as a model for planning future transient investigations or for possible fuel design modifications:

1. The neutron pulse supplied by the test reactor causes a release of energy from a portion of the fissile material present in the fuel. (The flux depression frequently present in the fuel results in maximum energy release at the fuel surface).
2. Fission fragments having a mean path length in UO_2 of ~5 microns deposit energy in surrounding fuel material (fission product spikes). This rise in energy content of the fuel is approximately uniform across the entire cross section of fuel save for the

effects of flux depression. It is superimposed on the previously existing temperature profile in the fuel (flat with no preceding power generation, otherwise approximately parabolic).

3. The rise in energy content of the fuel is evidenced as an equivalent rise in fuel temperature, tempered by the effects of:
   - variable specific heat
   - latent heat of fusion when the melting point is reached
   - latent heat of vaporization
   - heat of dissociation

4. The transient increases in fuel temperature result in the following:
   - heat flow from the hottest fuel to the clad and sometimes also toward the fuel centerline due to flux depression effects.
   - fuel volume increase due to thermal expansion, liquification, vaporization or gas release.
   - generation of thermal stresses in the fuel itself and accompanying or subsequent cracking.
   - possible changes in chemical equilibrium between fuel and gas phase.

5. The rate of heat flow to the fuel clad and, hence, the temperature gradient in the fuel clad can be extreme and result in thermal stresses well beyond the yield point. Such occurrences were considered in some detail in GEAP-4058 and appear consistent with findings in the present experiments. Therefore, they are not considered further here save to say that heat flow and thermal stresses per se should not (and did not) result in rupture of the fuel clad providing it remains in a ductile state and is adequately cooled externally.

6. Effects of volume increases in the fuel, although alluded to in the preceding analytical study, cannot be computed effectively. They have, however, shown up as one of the major effects causing fuel deformation in the present series of tests.

7. In the absence of restraint the fuel will expand freely as a result of the factors listed above. In practice, some degree of restraint is always present; frequently from the

clad and even from within the fuel itself. The cooler regions of the fuel tend to restrain expansion of the hotter central regions, and this restraint has been observed on many occasions to result in plastic flow of hot material. In the case of fuel of less than theoretical density (internal voidage), compression or collapse of the voids is also possible. Such plastic flow is temperature, as well as time and pressure dependent, and as such will be more evident in the hottest regions of the fuel, particularly in prolonged transients. (It is in fact directly akin to the sintering process.)

Plastic flow and densification (sintering) of the fuel during transients was clearly evidenced in the completed series of tests in at least three cases, namely:

Fig. 4-1, where "extrusion" of the fuel past the nickel ring in test 1-D, due to extreme volumetric expansion of the fuel body, carried the tungsten disk ahead of it.

Fig. 4-2, where a distinct barrel shape is evident in the fuel pellets which were originally centerless ground. This is believed due to compaction of the hot central cylindrical portion of the fuel, which on subsequent cooling would tend to pull the fuel into the barrel shape.

Fig. 4-3, where the radius of curvature of the fuel pellet surface following transient test 1-E is significantly less than in the "as fabricated" condition and less than that of the clad within which it was contained.

8. The time, temperature and pressure dependence of the plastic flow implies that during a given transient the fuel will expand as its temperature rises at a rate approaching that of unrestrained expansion, until such time as the fuel-clad gap is taken up and the clad or its equivalent is contacted. At this point the initial limited restraint, due to the cooler regions of fuel acting in tension, will be re-inforced by whatever strength the clad possesses.

9. Given sufficient clad strength and sufficient plasticity and void content in the fuel, there is evidence that further fuel expansion can be prevented.

10. In the absence of such conditions, further expansion of the fuel at a reduced rate is to be expected and will be accompanied by elastic, then plastic, deformation of the clad. (This will also be accompanied by improved heat transfer between fuel and clad.)

11. Plastic deformation of the clad will result in binding at fuel-clad interfaces with respect to relative translational movement and in consequence will tend to produce longitudinal stretching of the clad regardless of the presence or absence of longitudinal expansion spaces. (This occurrence is evidenced in test 1-E.)

12. For very rapid rates of power input, as would occur in a prompt power excursion in EFCR for instance, there will be a negligible time period available for plastic flow, and in consequence even the hottest UO_2 will tend to act as a rigid solid, thus producing maximum clad deformation.

13. Continued energy input to the fuel beyond that necessary to take the fuel to its melting point will result in melting of the fuel with no temperature increase in the melting zone, until such time as the full latent heat of fusion has been absorbed.

14. The large volume increase ($\sim 10\%$) associated with melting will give rise to significant local pressure generation and fuel movement during a transient. This is evidenced in test 1-D (Fig. 4-4) where UO_2 in a plastic condition has moved into the fuel-clad gap area.

15. Additional fuel movement due to slumping or draining of the molten UO_2 will also tend to occur and may be evidenced in test 1-D (Fig. 4-1).

16. Still further energy input to the fuel beyond melting will raise its temperature to levels at which its vapor pressure becomes appreciable. Considerable uncertainty exists as to the composition of the vapor which will be in equilibrium with high temperature UO_2. However, some degree of thermal decomposition is quite probable. Under circumstances in which some portions of the fuel material are hot enough to exert a vapor pressure in excess of the prevailing pressure in the capsule, boiling is to be expected and will result in vapor voids opening up within the liquid fuel mass, thus expelling it to lower pressure (cooler) regions. This is evicenced in test 1-D

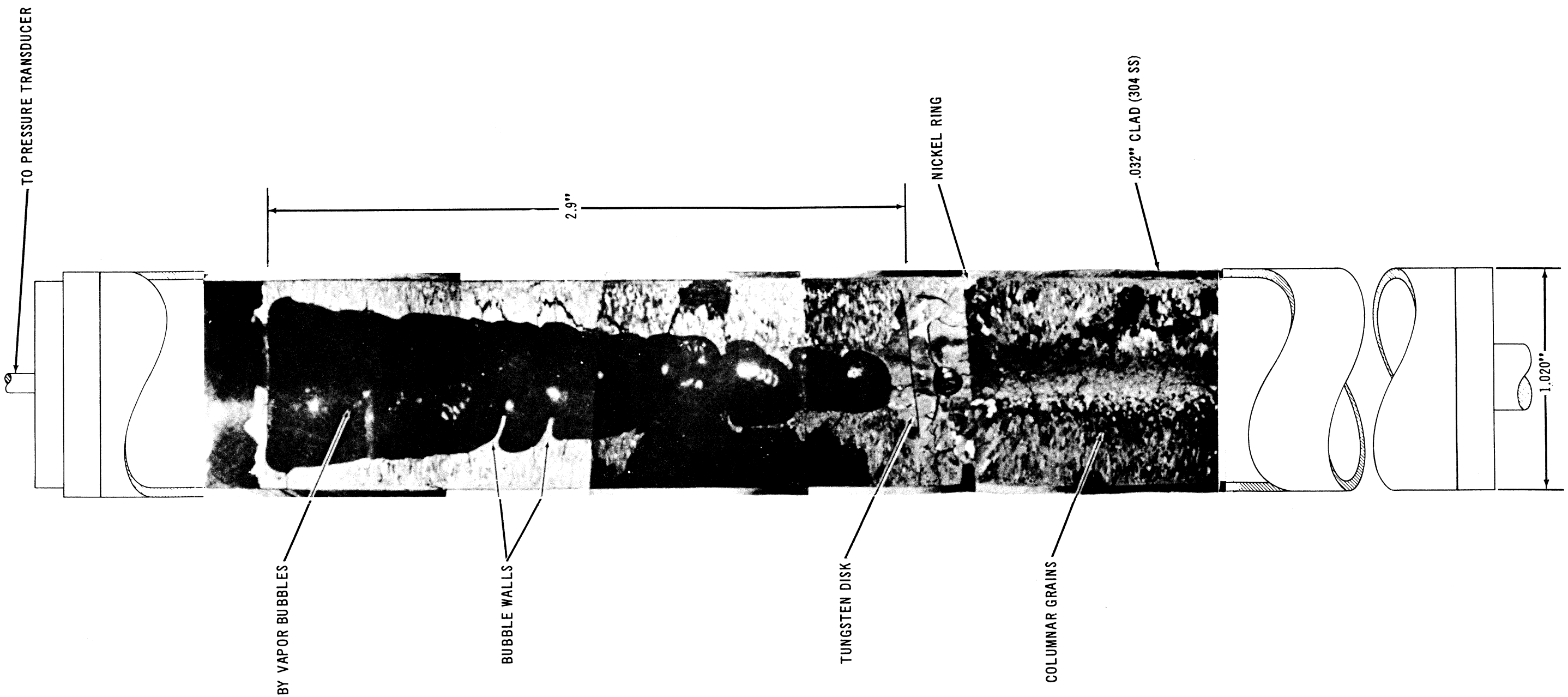

FIGURE 4-1 UPPER SECTION APED-TREAT SAMPLE 1D

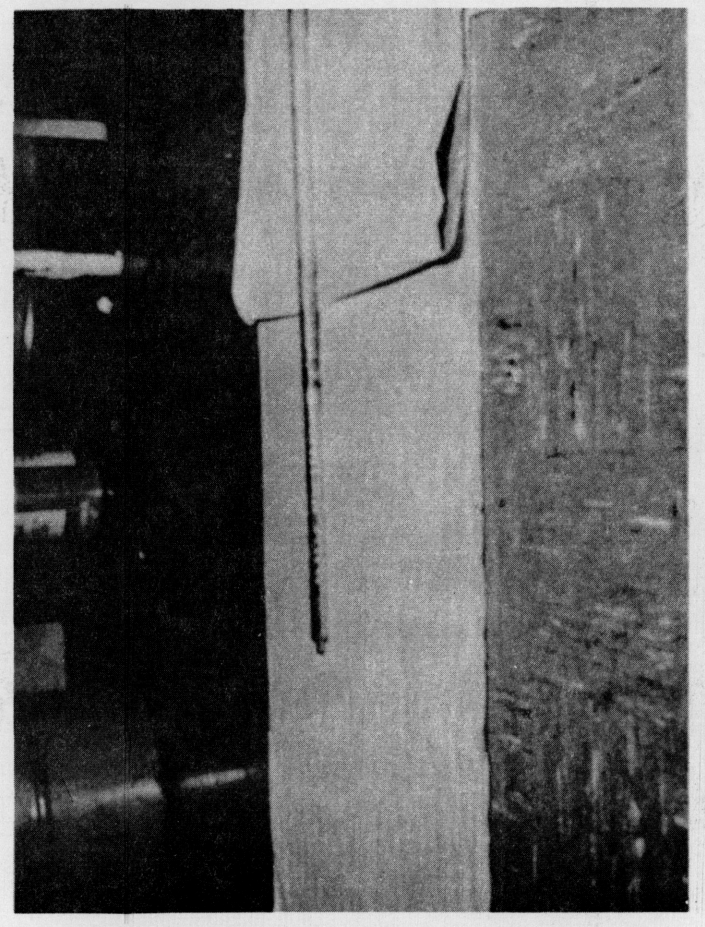

FUEL SPECIMEN AS REMOVED FROM CAPSULE

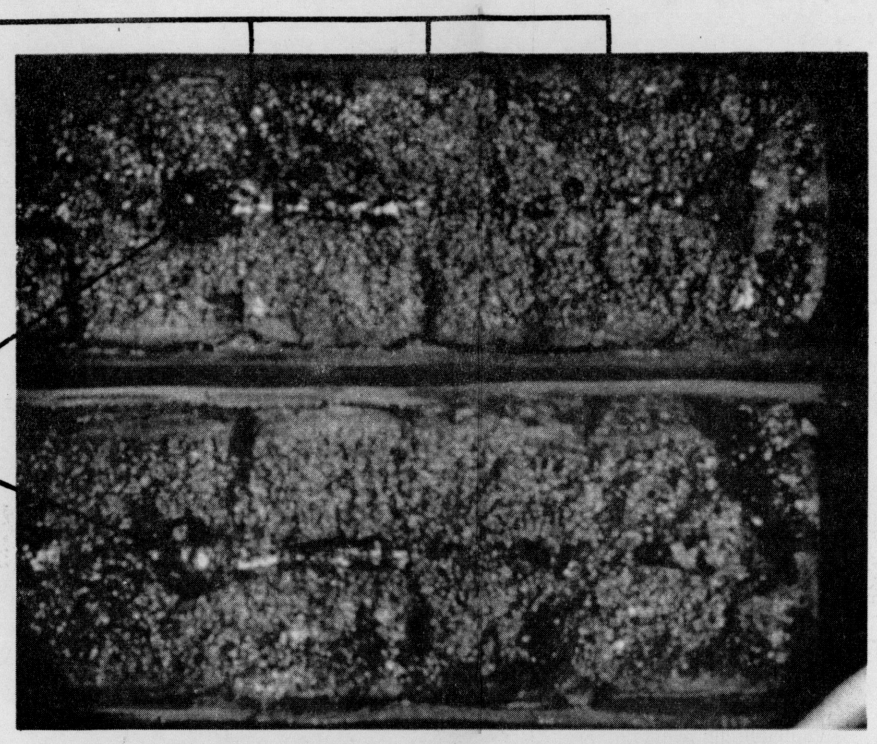

LONGITUDINAL SECTION

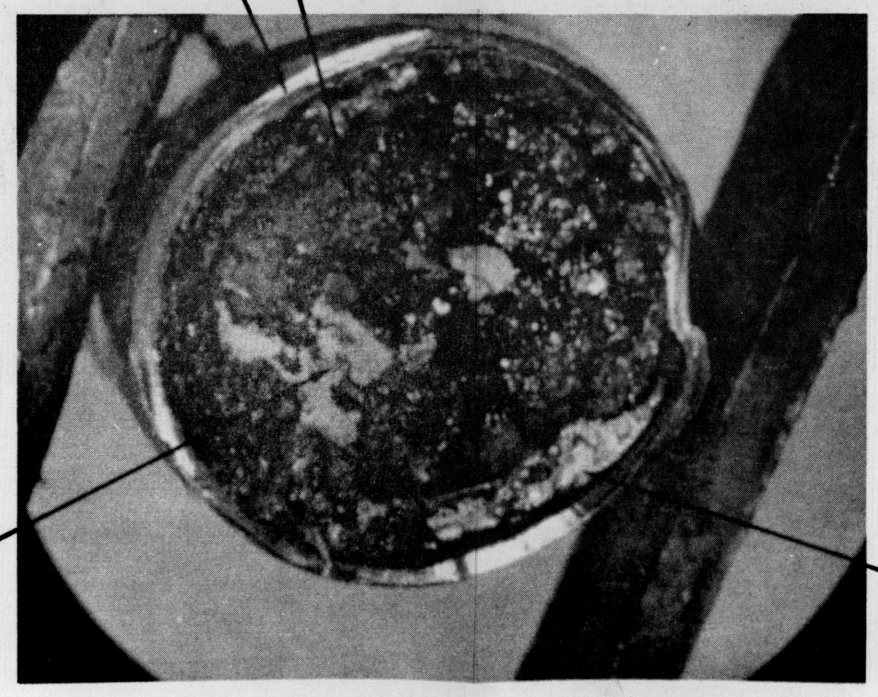

TRANSVERSE SECTION

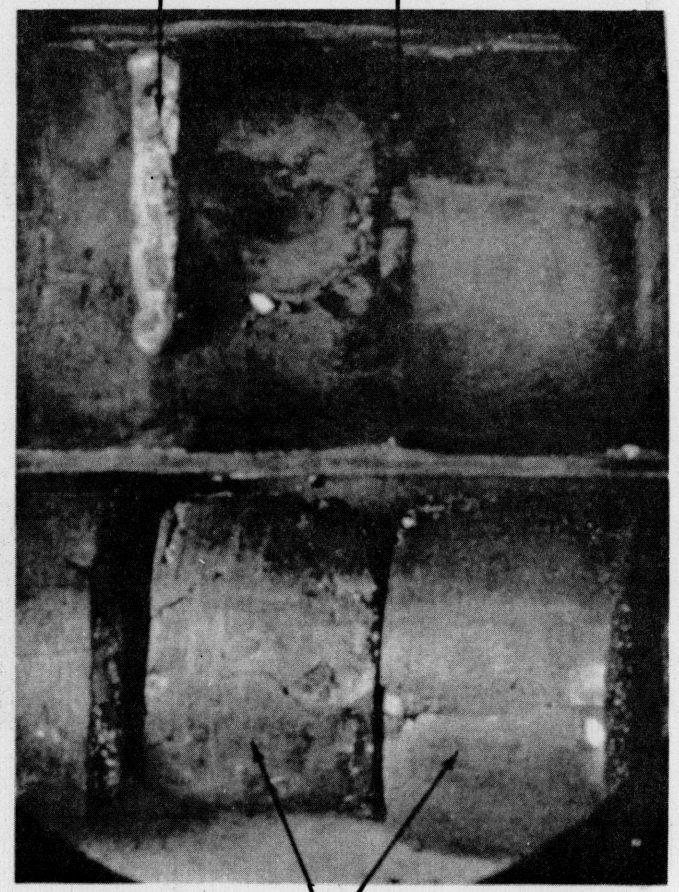

FUEL REMOVED FROM CLADDING

FIGURE 4–2 POST-IRRADIATION SECTIONING OF SAMPLE 1E

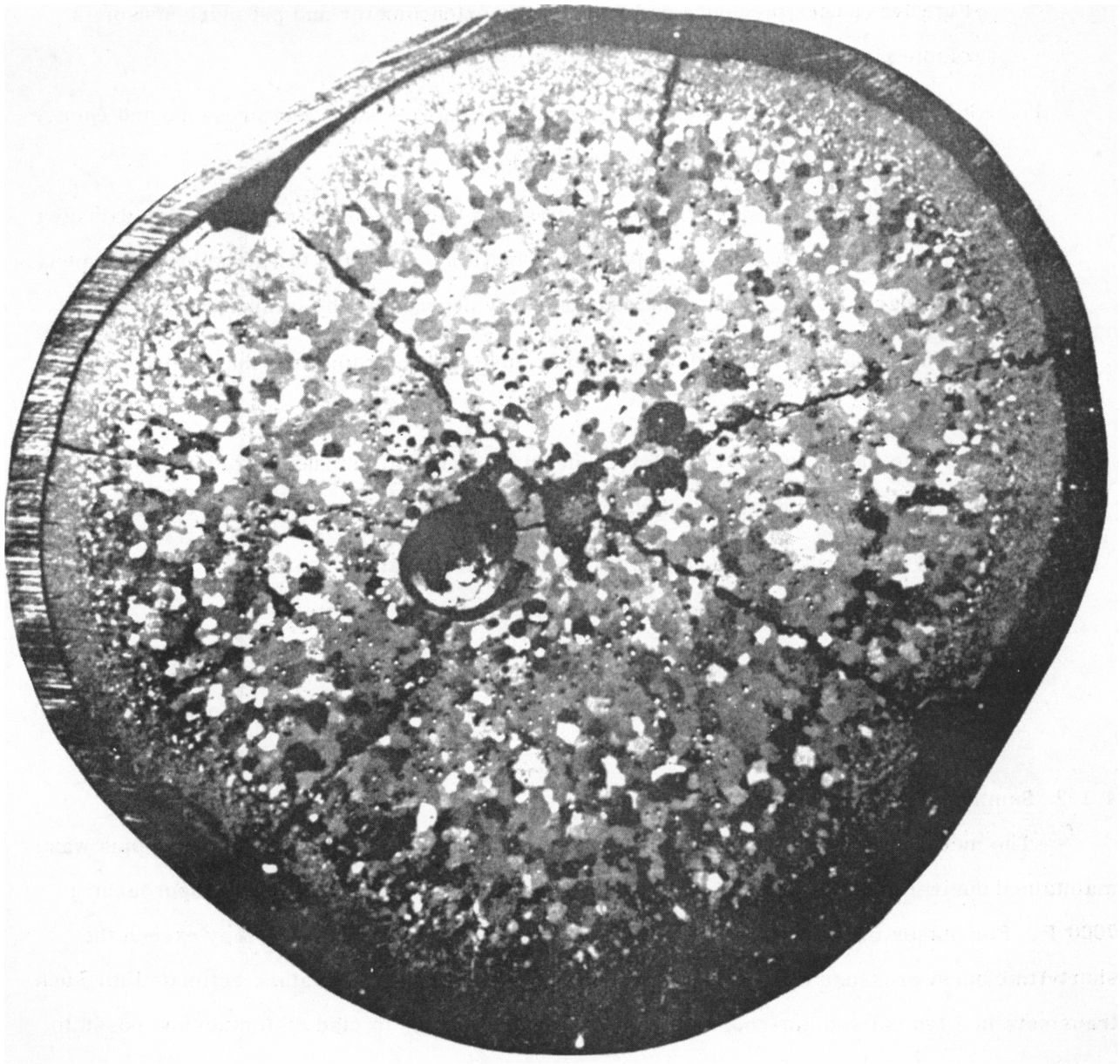

FIGURE 4-3 SAMPLE 1E POLISHED CROSS SECTION

(Fig. 4-5) where the upper end leads to the extensometer and pressure sensor (a volume sink).

17. Still further energy input can be expected to generate sufficient pressure and energy of expulsion to cause bursting of the fuel pin.

18. Any magnitude of power transient that results in non-elastic expansion and damage (e.g., cracking) to the fuel may, with repetition, give rise to ratcheting phenomena and progressive damage. Such damage may proceed by the following steps:

    a. The oxide fuel expands with temperature into the radial expansion space (Fig. 4-6).

    b. The fuel may tend to sinter, generating a central shrinkage void and a ring of high density material which resists inward expansion on the next transient.

    c. With successive transients the fuel moves outward to contact the clad and finally to deform it beyond its elastic limit.

    d. Fuel cracking and chipping may also produce mechanical ratcheting which will produce asymmetry and undulations in the cladding as seen in test IE (Fig. 4-3).

4.1.2 Summary of Conclusions from Series I Tests

The mechanical integrity of unirradiated stainless steel clad UO_2 Series I fuel pins was maintained during single power transients producing maximum fuel temperature approaching 7000 F. For higher maximum fuel temperatures the vapor pressure of UO_2 may exceed the short-time burst pressure of the clad at the ~1600 F mean wall temperature estimated for such transients in a typical sodium-cooled fast reactor, thus leading to clad distortion and possible rupture.

Over-all thermal expansion of the fuel in extreme single transients, was found to be a function of the internal spaces present in the system prior to the transient pulse. The proposed method of segmenting fuel internally was found to be successful in preventing clad deformation in single transients up to and slightly beyond the fuel melting point.

Repeated transients appear likely to cause inelastic clad deformation at a lower temperature than that for a single transient. This is believed due to a ratcheting mechanism in the fuel.

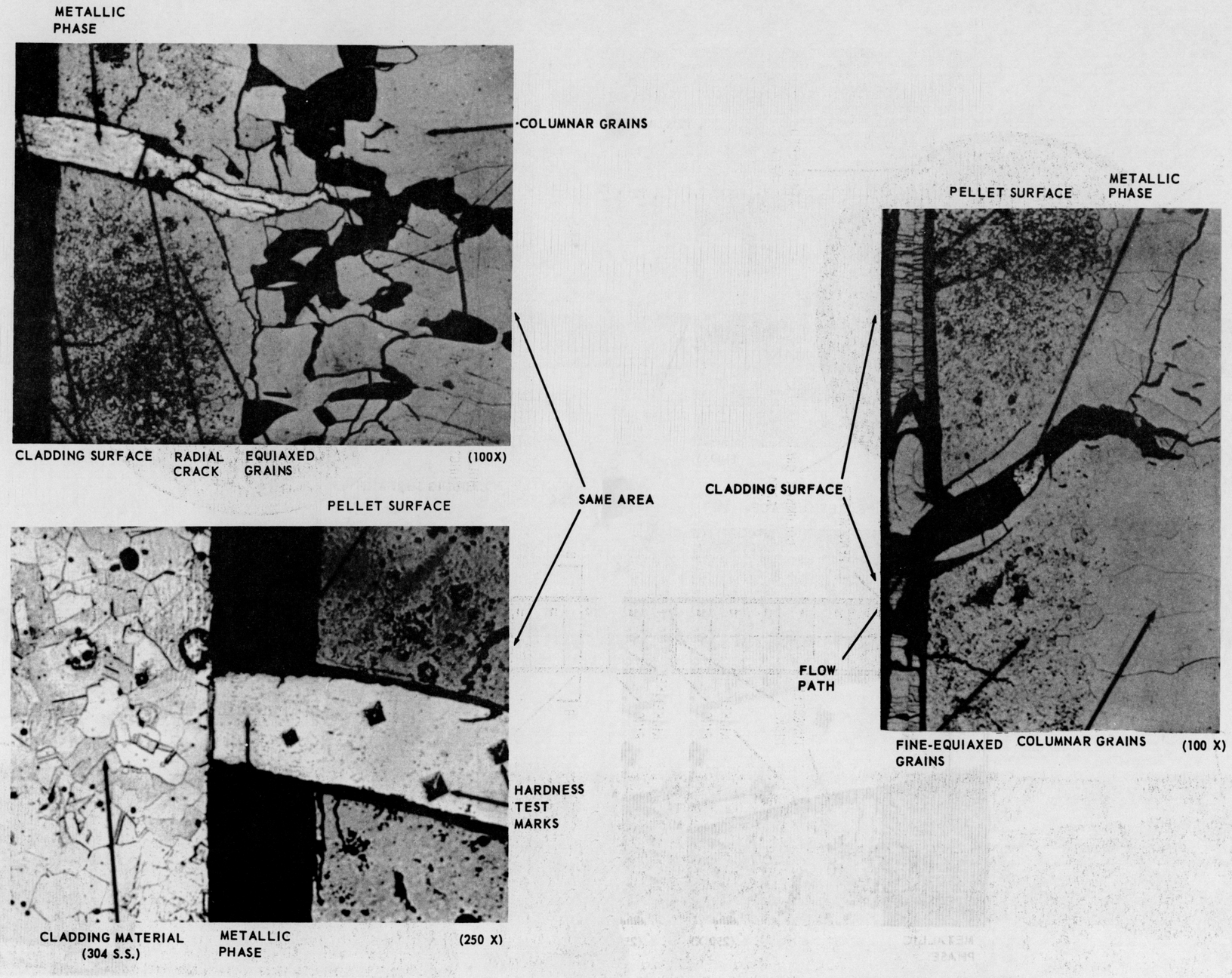

736-16

FIGURE 4-4 PHOTOMICROGRAPHS OF FUEL-CLAD INTERFACE – SAMPLE 1D

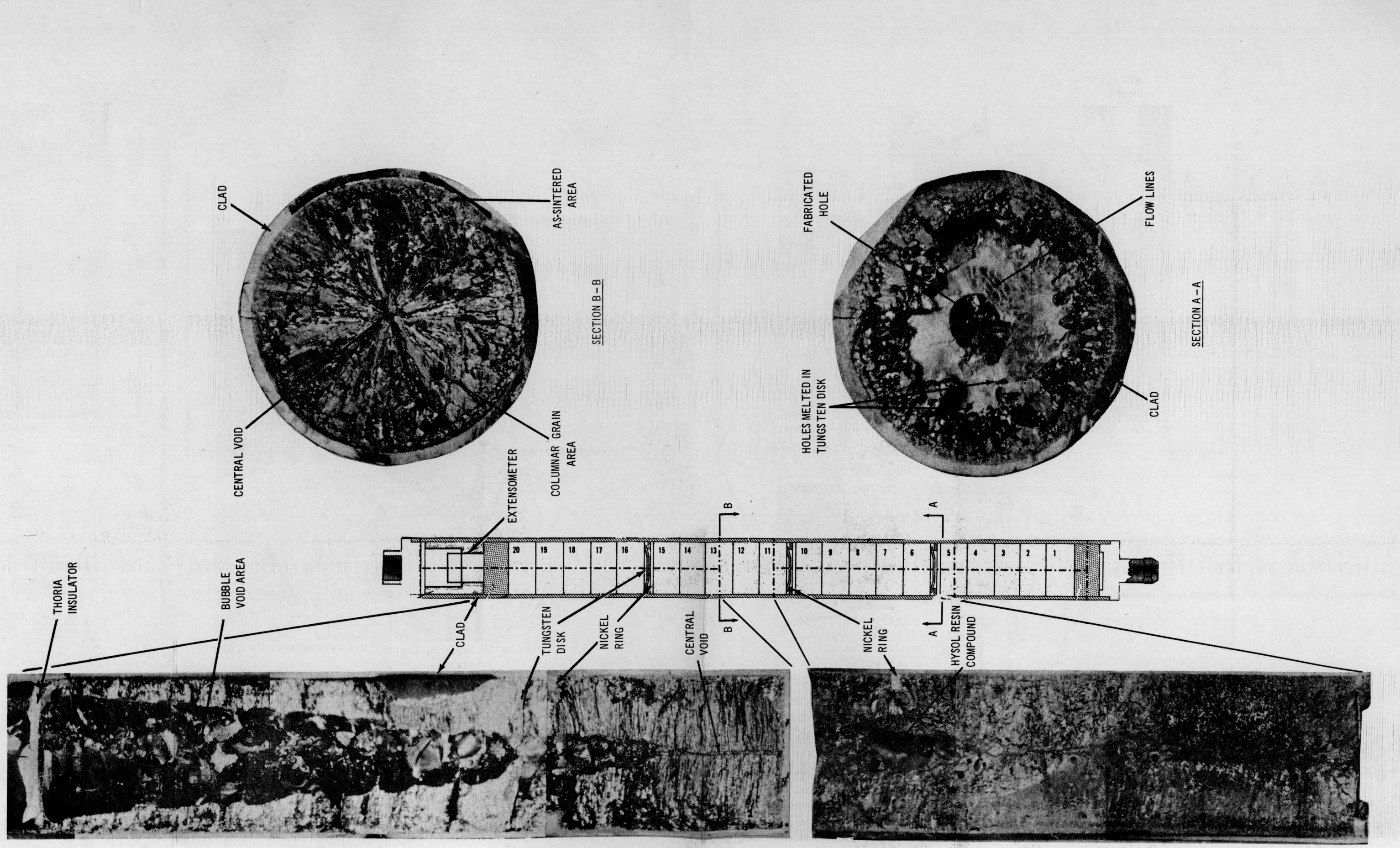

FIGURE 4 – 5 POST-IRRADIATION SECTIONING OF SAMPLE 1D

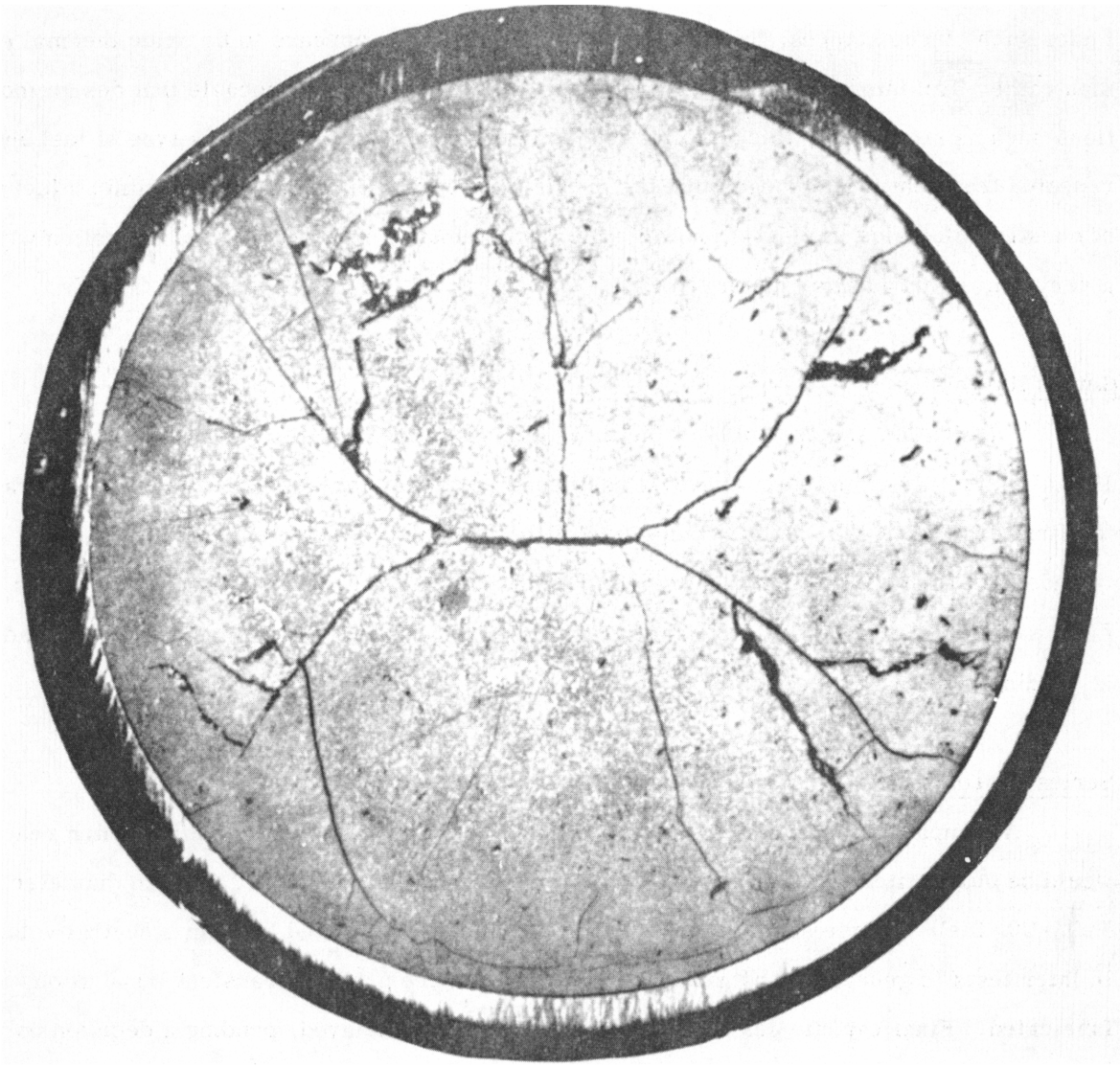

POST IRRADIATION TRANSVERSE SECTION

TREAT TRANSIENT POWER: 520 MW-SECONDS
GENERATED SAMPLE POWER: 238 ± 10 BTU/IN^3
ESTIMATED PEAK TEMPERATURE: 5220 ± 210 °F

FIGURE 4-6 APED – TREAT FUEL PIN 1C

Under such circumstances, the prime cause of clad damage appears to be oxide thermal expansion rather than internal gas or vapor pressure. It is considered probable that design modifications such as stronger or thicker clad would raise the failure limit for this type of fuel under repeated transients. It appears that the provision of radial expansion space within a fuel pin is of questionable value in view of probable fuel redistribution and central void formation with even a very limited irradiation history.

4.2 Series II Tests

Fabrication and assembly of the three Series II test capsules (0.25 inch diameter, 20% PuO_2-UO_2 fuel) is complete. Approval has been received from the TREAT facility to irradiate the first capsule (II-A). Thus, completion of the first test is expected in the near future. It is intended to reach the fuel melting region in the first transient test, with subsequent tests being more severe, to the point of incipient failure. Approval for the remaining Series II irradiations is pending, waiting the results of the first.

4.3 Series III Tests

A comparative study of GETR and MTR-ETR is underway to determine which reactor would be best suited for the Series III pre-irradiated test specimens (0.25 inch diameter, 20% PuO_2-UO_2 fuel). These specimens, which are to be pre-irradiated to form a central void, and in later tests to generate substantial fission gas pressure prior to transient irradiation, are now fabricated. Final capsule design and construction will be delayed, pending a decision on which reactor will be used for the pre-irradiations.

SECTION V

TASK D - MIXED CARBIDE FUEL STUDY

5.1 Comparison of Mixed Carbide and Mixed Oxide Fuel Cycle Costs

The second part of the topical report, GEAP-3880. Comparative Study of PuC-UC and PuO_2-UO_2 as a Fast Reactor Fuel. Part II - Economic Considerations, has been written and issued. Part I of this report, issued previously, evaluated these two ceramic fuel alternatives on the basis of the principal technical considerations: ceramic fuel properties, heat transfer, fluid dynamics, and nuclear performance. On the basis of preliminary assumed unit costs, Part I indicated that the technical superiority of carbide could result in a potential fuel cycle cost advantage of 0.26 mills/kwh. Part I also outlined the major developments in technology which would be necessary to achieve this potential. Substantial development effort is indicated in the areas of fabrication processes, cladding and fuel compatibility, the effects of plutonium content and burnup on thermal conductivity and density of the mixed carbide, and thermal stresses in the clad.

Part II of GEAP-3880 extends the comparison to include the fuel cycle cost analysis in greater detail, particularly with respect to fabrication and reprocessing costs. Two separate cases for carbide fuel are considered, each of which exploits the superior thermal conductivity and higher fuel density of carbide in a different way. Comparative fuel cycle costs for the two carbide designs and the reference oxide design (GEAP-3721) are summarized in Table V-1.

In the case referred to as the Reference Carbide Design, the properties of carbide have been used to increase the linear power generation in the core rods by a factor of four by increasing both the core rod diameter and the core fuel specific power. In the case of the Alternate Carbide design, carbide is substituted for oxide using approximately the same rod diameters, fuel specific power, and core loading. The result is a higher breeding ratio, but also higher fabrication costs. Hence the relative fuel costs will depend upon the value assigned to plutonium.

TABLE V-1

FUEL CYCLE COST BREAKDOWN

1975 Economic Basis	Reference Oxide	Reference Carbide	Alternate Carbide
Fabrication	0.28	0.30	0.33
Reprocessing	0.22	0.22	0.22
Fuel Inventory	0.34	0.24	0.32
Plutonium Credit	(0.16)	(0.22)	(0.22)
First Core Fabrication Capital	0.11	0.09	0.15
Total, mills/kwh	0.79	0.63	0.80
1980 Economic Basis			
Fabrication	0.28	0.30	0.33
Reprocessing	0.17	0.17	0.17
Fuel Inventory	0.62	0.44	0.58
Plutonium Credit	(0.30)	(0.41)	(0.41)
First Core Fabrication Capital	0.11	0.09	0.15
Total, mills/kwh	0.88	0.59	0.82
Bases			
Fabrication, $/kg U + Pu	76	88	96
Core Specific Power, kw/kg U + Pu	128	172	128
Breeding Ratio	1.19	1.27	1.27

Factors Common to all Three Designs	1975	1980
Reprocessing Throughput, tons/yr	75	250
Reprocessing Cost, $/kg U + Pu	62	49
Plutonium Value, $/g Pu-239 and -241	6.60	12.00
Carrying Charge, %/yr	10	10
Plant Load Factor	0.8	0.8

All three designs (the two carbide cases and the base oxide case) have the same overall core and blanket region dimensions but the Reference Carbide design produces 50% more power than either of the other two. The breeding ratio is the same as the Alternate Carbide Design, but both fabrication and inventory costs are reduced. The Reference Carbide design results in the lowest fuel cost of the three with the advantage increasing in direct proportion to the assigned value of plutonium.

The comparison on the 1975 economic basis as given in Table V-1 is somewhat less favorable to the carbide cases than was predicted in Part I, the change being attributed for the most part to an increase in the estimated cost of carbide fuel fabrication relative to that of oxide fuel as evidenced by the detailed fabrication cost estimate. There have also been incorporated in the fuel cycle cost breakdown the latest results on reprocessing economics and physics.

To realize the limited cost saving potential of carbide fuel will require operation at fuel and cladding ratings beyond the reach of present technology. Clearly the 0.16 mill carbide fuel margin shown for 1975 operation is insufficient to warrant a change in direction of development from the relatively well matured oxide technology for the first developmental FCR plants.

5.2 Carbide and Oxide Reactor and Fuel Designs

Major features of the two carbide and reference oxide reactor and fuel designs, on which the foregoing fuel cycle cost estimates are based, are given in Table V-2.

In this comparative study, the following reactor and fuel design features were held constant for the three designs:

1. Sodium coolant outlet temperature;
2. Plant thermal efficiency and load factor;
3. Of the total power, 86% is generated in the core, 8.1% in the axial blankets, and 5.9% in the radial blanket;
4. Diameter and active height of the core fuel zone and axial blankets;
5. Length of fission product gas plenum at the top of the core fuel rods;

TABLE V-2

REACTOR AND FUEL DESIGN PARAMETERS

		Reference Oxide	Reference Carbide	Alternate Carbide
Output				
Core		1200	1800	1195
Axial Blanket	MW	113	169	113
Radial Blanket	MW	82	123	82
Total Thermal	MW	1395	2092	1390
Thermal Efficiency	%	37	37	37
Net Electric	MW	517	775	515
Core				
Fuel Material		PuO_2-UO_2	PuC-UC	PuC-UC
Enrichment	% Fiss. Pu	12.8	11.5	11.5
Fuel Weight	MT(U+ Pu)	9.38	10.42	10.40
Specific Power	kw kg Fiss. Pu	1000	1500	1000
Specific Power	kw/kg U+Pu	128	172	115
Exposure	GWD/T*	100	100	100
Clad Material		SS	SS	SS
Clad Thickness	in.	0.015	0.0225	0.015
Rod OD	in.	0.25	0.37	0.24
No. of Rods		40.640	15,800	37,850
Fuel Length	ft.	3.25	3.25	3.25
Plenum Length	ft.	2.9	2.9	2.9
Fuel Density	gm/cc	10.4	12.8	12.8
Axial Blanket				
Material		UO_2	UC	UC
Enrichment	%	depl.	depl.	depl.
Weight	MTU	7.21	8.03	8.00
Exposure	GWD/T*	12.2	12.2	12.3
Clad Mat. Thkness.	OD, No.	Same as respective Core		
Fuel Length	ft.	2 × 1.25	2 × 1.25	2 × 1.25
Radial Blanket				
Material		UO_2	UO_2	UO_2
Enrichment	%	depl.	depl.	depl.
Weight	MTU	22.3	22.3	22.3
Exposure	GWD/T*	2.85	3.20	3.20
Clad Material		SS	SS	SS
Clad Thickness	in.	0.015	0.015	0.015
Rod OD	in.	0.45	0.45	0.45
No. of Rods		20,130	20,130	20,130
Fuel Length	ft.	4.5	4.5	4.5
Overall Length	ft.	5.0	5.0	5.0
Fuel Residence Time	yrs.	2.95	2.19	3.29
Breeding Ratio		1.19	1.27	1.27

* 10^9 watt-days per 2000 lb. U+Pu

6. The radial blankets are identical in all respects, including fuel material (UO_2); rod diameter, plenum and fuel lengths, blanket thickness and rod spacing;

7. Steel to fuel ratio in core and blankets;

8. Core fuel burnup.

The Alternate Carbide design corresponds to the Reference Oxide design in rod diameter, linear power generation, and specific power, so the comparison with oxide shows differences due only to substitution of carbide for oxide in the core and axial blanket. Although, for equal burnup, carbide fuel has better neutron economy, the increased fabrication cost results in higher fuel costs than oxide.

In the Reference Carbide design the linear power generation is increased to a maximum of 74 kw per foot of core fuel length, compared to 18 kw per foot for the other two cases. This is the combined effect of two changes:

1. Increasing fuel specific power, which reduces inventory charges, and

2. Increasing core fuel rod diameter which reduces fabrication costs.

The Reference Carbide design concept makes heavy demands upon the fuel cladding which cannot be met with assurance using today's materials and design practices. The following key developments must be achieved:

1. A fuel design which assures low contact resistance to heat transfer at the fuel clad interface. The design must be compatible with a fuel exposure of approximately 100 GWD/T and temperatures of approximately 1500 F at the fuel outside diameter, and 3500 F or more at the center.

2. A fuel clad which can simultaneously operate at up to 3×10^6 Btu/hr ft^2 and retain fission gas pressure, while having neutron absorption characteristics not significantly worse than stainless steel in the FCR core flux.

3. The clad must be compatible chemically with carbide and other materials of its environment.

SECTION VI

TASK E - FUEL PERFORMANCE EVALUATION

6.1 Scope and Objectives

The objective of Task E is the development and evaluation of fuel meeting the performance objectives* of an economically viable fast reactor.

Effort this quarter was redirected to five sub-tasks with the following general objectives:

1. Measurement of temperature distributions and effective conductivity of mixed oxide fuel at low and high irradiation levels.
2. Irradiation testing of well-characterized fuel of controlled stoichiometry to high burnup.
3. Determination of plutonium mobility at high temperatures in mixed oxide fuel to anticipate possible migration or segregation effects which could influence the kinetics and magnitude of the Doppler effect.
4. Determination of fuel composition and properties with primary emphasis on the determination of stoichiometry in fabricated and in irradiated fuel, and observation of the effects of macroscopic concentrations of fission products on properties.
5. Experimental fuel fabrication development including reduction-to-practice of reference processes for producing fuel bodies of controlled stoichiometry and physical characteristics, and including preparation of compactible high density power by a direct sintering process.

The work on items (1), (2), and (4) above was initiated during this quarter; items (3) and (5) are continuations and extensions of work from prior quarters.

---

* The performance objectives for Task E are those limited to normal operating conditions. Behavior of fuel under unusual conditions, such as transients or defects, is investigated under Tasks B and C.

6.2 Thermal Properties

The variation in conductivity of PuO_2-UO_2 fuel with O/M ratio and with irradiation history affects fuel temperature and is important in determining the Doppler Δk available in an operating reactor. Usual temperature-sensing elements have short lifetimes at the central temperatures desired for high performance fuel. Design of experiments to test the compatibility of temperature-sensing elements with UO_2-PuO_2 is in progress for use in short-term temperature and conductivity measurements.

Gas thermometry is being investigated for use in long-term irradiations. Calculations of transducer sensitivity to temperature as a function of initial filling pressure and to the system volumes have been made. Table E-1 summarizes the sensitivity calculations for one temperature. Concept design of a capsule with two pins and two gas pressure transducers has been prepared. Components of this design are being procured for testing.

TABLE E-1

GAS THERMOMETER SENSITIVITY AT 4000 K

V_2/V_1	T_2	P/P_o	dP/dT; psi/°K $\times 10^3$
0.2	350	4.18	0.317
0.1	350	5.87	0.687
0.1	575	6.78	0.998
0.0067	350	6.92	0.982

V_1 is volume of gas bulb at 4000 K. V_2 is volume of transducer and lead tube. T_2 is temperature in °K of V_2. P_o is the initial filling pressure.

6.3 High Burnup Fuel

Capsules and pins for the irradiation of mixed oxide fuels of controlled stoichiometry are being designed. In order to permit intelligible correlations of fuel behavior, it is essential to provide a known and controlled flux and temperature environment. Analysis of peak and average

linear power generation available in GETR as a function of spike enrichment and diameter of pin is given in Table E-2.

A minimum four-week-cycle variation of about 15 percent in local flux is available for a preferred location near the mid-plane. Long-term variation in heat generation rate due to fuel burnup is minimized by using about 40 percent spike enrichment of uranium-235 in addition to 20 percent plutonium.

TABLE E-2

LINEAR POWER GENERATION

20% PuO_2-UO_2 Pins

GETR Location	Diameter, Inches	Spike Enrichment, % U-235	Linear Power, kw/in	
			Average	Peak, Start of Cycle
Pool	0.15	0.7	1.26	1.73
	0.15	20	1.45	1.99
	0.15	40	1.54	2.11
	0.15	100	1.64	2.25
	0.25	0.7	1.80	2.46
	0.25	20	1.97	2.71
	0.25	40	2.06	2.82
	0.25	100	2.16	2.96
Core	0.15	0.7	3.77	5.43
	0.15	20	4.42	6.36
	0.15	40	4.74	6.81
	0.15	100	5.08	7.31
	0.25	0.7	5.66	8.14
	0.25	20	6.27	9.02
	0.25	40	6.56	9.44
	0.25	100	6.92	9.95

Fuel positioned 3 to 23 inches above GETR core bottom average.

Maximum gamma heating in pool - 1.8 watts/g

Maximum gamma heating in core - 8.6 watts/g

Preliminary physics and heat transfer analysis has been made of a parallel-pin capsule configuration to permit irradiations of three compositions simultaneously. Convection flow heat-transfer yields sodium velocities of 0.4 feet per second without boiling. More nearly isothermal operation is attainable by permitting sodium (or NaK) boiling. The self-shielding for three pin arrays has been calculated for two pin diameters and as a function of reactor position and uranium-235 spike added. Azimuthal surface flux dependence was derived by making a solid angle correction for the equivalent annual fuel element. Table E-3 summarizes the results of this calculation.

TABLE E-3

FLUX DEPRESSION FACTORS FOR THREE-PIN ARRAY*

GETR Location	Diameter, Inches	Spike Enrichment, % U-235	Φ_c/Φ_o	Φ_i/Φ_o
Pool	0.15	0.7	0.59	0.63
	0.15	20	0.41	0.48
	0.15	40	0.28	0.39
	0.15	100	0.11	0.28
Core	0.15	0.7	0.64	0.68
	0.15	20	0.46	0.52
	0.15	40	0.33	0.43
	0.15	100	0.13	0.30
Pool	0.25	0.7	0.38	0.45
	0.25	20	0.22	0.33
	0.25	40	0.13	0.28
	0.25	100	0.04	0.24

* Φ_c/Φ_o is flux ratio of pin center to outer pin surface. Φ_i/Φ_o is flux ratio for inner pin surface to outer pin surface. Three 0.15 inch pins with centers equally spaced on a 0.30 inch diameter circle; or three 0.25 inch pins centered on a 0.47 inch diameter circle.

6.4 Plutonium Migration

In addition to surveillance of scheduled irradiations, two alternate plutonium migration experiments are being analyzed:

a. Axial migration, isothermal but with uranium and plutonium concentration gradients,

b. Axial migration, isothermal and constant composition, using plutonium-242 as tracer for plutonium self-diffusion.

The mobility of plutonium (as well as of uranium and of oxygen) in an oxide lattice is expected to be a function of stoichiometry as well as temperature. Commitment of specific migration or segretation experiments is being deferred until next quarter when more results are available from the sub-tasks on fuel temperature measurement on stoichiometry.

6.5 Fuel Composition and Properties

Installation of equipment for the more accurate and convenient gravimetric analysis of mixed oxides is nearing completion. A tungsten resistance furnace has been adapted for use with reducing or inert atmospheres with controlled water vapor content for a program to determine the effects of sintering variables on stoichiometry and physical characteristics of the oxide. The oxygen to plutonium ratio in plutonium oxide which was fired under reference sintering conditions as given in Table E-4 was observed to be 1.852 ±0.003.

TABLE E-4

REFERENCE PELLET-SINTERING PROCESS

Furnace temperature	1575 ±25 C
Nominal gas composition	6% H_2, 94% He
Initial water content of gas	ca. 100 ppm
Gas flow rate	10 cu ft/hr
Total gas pressure	1 atm.
Furnace loading	ca. 40 g
Reaction time	4 hours

This value was obtained on duplicate 0.22 inch OD pellets by a method which assumes the material after heating in air at 900 C to constant weight is $PuO_{2.000}$. This stoichiometry observed for plutonium oxide is in excellent agreement with that calculated from the thermodynamics of the reaction

$$2\ PuO_2 + H_2 = Pu_2O_3 + H_2O$$

Based upon this observed behavior for plutonium oxide, and upon the previously observed reduction of uranium dioxide to $UO_{2.006\ \pm 0.003}$ when sintered under similar conditions, it may be calculated that mixed oxide pellets containing 20 per cent plutonium oxide sintered under the reference conditions will have the composition

$$O/(U + Pu) = 0.8(2.006) + 0.2(1.852) = 1.975$$

assuming that the components of mixed material behave like the separate oxides.

A second batch of plutonium oxide was prepared via the Pu(IV) oxalate route in order to have material in readiness for further fuel property studies.

6.6 Experimental Fuel Fabrication

6.6.1 Pellet Fabrication

6.6.1.1 Preparation of Mixed Oxide Powder for Pelletizing

Three batches of mixed oxide powder were processed in accordance with the reference process as detailed in "FCR-Mixed Oxide Fuel Specification No. FCR-1F". Batch weights and compositions were as follows:

Batch No.	SS Wt., g	% Pu	% Natural U
B-6	200	22.5	77.5
B-7	300	19.7	80.3
B-8	250	≈20.0	≈80.0

Powder batches B-6 and B-7 were used to produce pellets with uniform shrinkage and specification densities: therefore, the powder was apparently of good ceramic quality.

6.6.1.2 Pellet Pressing and Sintering

Mixed oxide powder from Run B-6 (22 per cent plutonium - 78 per cent natural uranium) was utilized to evaluate various types of sintering cycles. Pellets were pressed at pressures of 10,000 to 44,000 psig and were fired at 1410 to 1580 C for one to four hours. Significant data are presented in Table E-5.

Rapid heating and cooling (pellets placed directly into hot zone of furnace, approximately 1300 C, and removed from hot zone, approximately 1500 C, without prior cooling) resulted in warped pellets with very low apparent densities (Pellets B-6-67 through 72; 86.4 to 88.6 per cent of theoretical). Sintered density appeared to vary directly with sintering temperature with higher densities attained at higher temperatures. Time at sintering temperature appeared to have little further effect on sintered density after two hours.

Pellets receiving essentially identical treatment (pressed and fired at same conditions and at same time) had significantly different sintered densities (differences up to 4.2 per cent of theoretical). This variation appears to be due to a temperature gradient during the sintering cycle since densities are frequently different for pellets in the rear of the furnace boat as compared to those in front. Future investigations will include a study of temperature or atmosphere gradients within the firing zone of the furnace as well as additional studies of sintering parameters.

Conclusions from the foregoing tests (Table E-5) are as follows:

a. Sintered density did not appear to vary with pelletizing pressure or green density within the range investigated (10,000 to 28,000 psi and 46 to 52 per cent theoretical density).

b. Rapid heating and cooling during firing (pellets placed directly in hot zone of furnace, approximately 1300 C, and removed from hot zone, approximately 1590 C, without prior cooling) resulted in warped pellets with low apparent densities (86 to 89 per cent of theoretical).

c. Sintered density appeared to vary directly with sintering temperature over the range 1410 to 1580 C, for pellets green pressed at 11,500 psi.

TABLE E-5

PRESSING AND SINTERING DATA FOR POWDER BATCH B-6

22% Pu - 78% Natural U Mixed Oxides

Pellet No.	Pelletizing Pressure (psig)	Green Density (% Theoretical)		Sintering		Sintered Density (% Theoretical)				Comments
		Range	Avg.	Temp.(1) (°C)	Time (hrs.)	Range	Avg.	Diametric	Axial	
1- 4	10,000	46.0-46.2	46.1	1520-1560	4	94.2-95.2	94.6	22.3	21.1	
5- 8	15,000	48.3-48.9	48.6			94.1-95.6	94.7	21.0	19.9	
9-12	20,000	50.3-51.1	50.9			94.5-96.0	95.3	20.0	18.5	
13-16	10,000	45.1-46.2	45.8	1520-1570	4	93.5-94.6	94.1	22.2	21.2	
17-20	15,000	48.2-48.7	48.5			94.4-94.6	94.5	21.0	19.7	
21-24	20,000	49.0-51.1	50.4			94.0-94.8	94.4	20.3	18.2	
25-27	11,000	46.3-47.1	46.8	1500-1550	4	93.2-95.8	94.9	21.9	20.8	
28-30	12,500	47.7-47.9	47.8			91.5-93.0	92.3	20.8	19.1	
31-33	15,000	48.2-49.4	48.9			95.1-96.0	95.7	20.8	19.7	
34-36	17,000	49.8-50.1	50.0			90.8-94.4	92.7	19.8	18.4	
37-39	11,500	46.9-47.2	47.0	1530-1550	4	94.9-95.7	95.2	22.0	21.1	
40-42	20,000	46.2-46.4	46.3			93.8-95.3	94.6	19.9	18.6	
43-45	28,000	53.0-53.7	53.4			94.7-94.7	94.7	18.6	17.3	
46-48	44,000	55.3-56.2	55.8			92.3-93.9	93.1	16.8	15.5	Warped(2)
49-54	12,000	47.1-47.4	47.2	1500-1530	4	92.0-95.9	94.2	21.5	20.3	
55-60	11,500	46.8-47.4	47.0	1450-1470	4	92.5-94.5	93.0	21.4	20.3	
61-66	11,500	46.1-48.2	46.9	1420-1440	4	92.2-94.2	93.4	21.6	20.5	
67-72	11,500	46.3-47.1	46.8	1530-1550	4	86.4-88.6	87.0	20.4	17.7	Rapid Heating(3) Pellets Warped(2)
73-78	11,500	46.2-46.8	46.7	1410-1440	4	90.5-93.6	91.7	21.1	19.9	
79-84	11,500	46.4-47.3	46.9	1530-1550	3	94.8-96.4	95.8	22.0	20.9	
85-90	11,500	47.1-48.0	47.4	1550-1570	4	93.9-96.3	95.2	22.1	20.4	
91-96	11,500	46.2-47.2	46.7	1510-1540	2	91.5-95.7	94.0	21.7	20.5	
97-102	11,500	46.4-47.3	46.8	1540-1580	1	91.1-92.2	91.4	20.9	19.7	

NOTES: (1) Average of front and rear of boat.

(2) Hour-glass configuration.

(3) Boat charged directly into 1300 C section of furnace.

d. Significant variations in sintered densities (up to 4.2 per cent of theoretical) within groups of pellets receiving essentially identical treatment (pressed and fired at same conditions and at same time) appeared to be due to a temperature gradient across the furnace boat during firing. Closer control of boat position within the firing zone appears to result in more uniform densities. Furnace atmosphere and quantity of pellets fired at one time appear to be significant variables and are under investigation.

e. There appeared to be no significant variation in sintered density with variations in time at firing temperature from two to four hours. A one-hour period at firing temperature resulted in significantly lower density.

6.6.2 Preparation of Mixed Oxide Powder for Vibratory Compaction

High density mixed oxide powder may be prepared by sintering compacts made from co-precipitated ammonium diuranate and plutonium hydroxide. A series of experiments designed to optimize the precipitation variables indicated that a pH of 9 or higher, at a temperature of either 20 C or 60 C, was desirable to give maximum final densities. The time of digestion appeared not to be important within the 10-30 minute range studied.

Using conditions that were previously determined to be optimum (i.e., pH = 9, temperature of digestion 60 C) a forty-gram heavy element batch of 20 per cent plutonium - 80 per cent uranium composition was precipitated. This material, when dried, pressed, and sintered at 1475 C for four hours in 6 per cent hydrogen - 94 per cent helium, yielded mixed oxide with a 10.7 density. This result is in agreement within 95 per cent confidence limits of that predicted by the statistically derived function. This material is being crushed, ground, and classified into particle size fractions desired for vibratory rod filling in order that a test may be made of the compacted density obtainable.

6.7 Plutonium Laboratory Operations

One 159 gram batch of plutonium nitrate was received from Hanford and a second batch was requested. License limitations continue to restrict full utilization of the facility. A license amendment (Amendment No. 15, License No. SNM-206) increasing plutonium limit to 1500 grams, was submitted to USAEC-WASH licensing personnel for approval.

Six hundred grams of fully-enriched uranium dioxide were received from Lawrence Radiation Laboratory. Excess and waste mixed oxide powder and pellets, containing 89 grams of plutonium, from the FOB program and the current development program were shipped to the Oak Ridge National Laboratory per ORNL request.

The Laboratory Safeguards Group approved revised procedures including:

a. Storage facilities for mixed oxides,

b. Facility for oxygen-to-metal and melting point determinations,

c. Temporary welding facility for long pins, and

d. Use of sodium in special fuel pins and in sodium-fuel compatibility tests.

Apparatus for flash melting of fuel on a tungsten ribbon is nearly completed. The components for x-ray crystallography and fluorescence analysis on plutonium samples were received and installed during the period.

Specification FCR-1F was issued. This specification defines materials, reference process, and quality requirements for mixed oxide pelletized fuel and fuel specimens for the FCR experimental program.

SECTION VII

TASK G - REACTOR DYNAMICS AND DESIGN

7.1 Updating FCR Reference Design

7.1.1 Summary

Recalculation of the physics parameters of the earlier reference design[1] in light of new cross-section data and improved calculation methods has been completed. The new cross-section data requires a new reference design point, since the reference design based on the old cross-section set, when evaluated using the new set, shows:

a. A hardening of the spectrum, which results in improved neutron economy and reduction of the Doppler coefficient, and

b. A positive reactivity change upon total loss of coolant.

Modifications of the core design and/or of operating conditions to achieve the necessary balance between the fuel economics and the safety parameters are being evaluated. These include:

a. Adjusting the fuel and sodium volume fractions to achieve a zero reactivity change with total loss of sodium.

b. Operating at lower specific power and, hence, lower fuel temperatures to increase the Doppler effect and decrease operating reactivity required for burnup.

c. Introducing moderating material into the core to degrade the spectrum and thereby increase the Doppler effect.

d. Changing the size and shape (L/D) of the core and investigating other possible core and blanketing configurations.

e. Sodium bonding or otherwise improving the fuel element heat transfer characteristics to permit a lower fuel temperature and, hence, a higher Doppler effect for a given rod power.

Combining items a. and b., above, for example, it has been found that a zero reactivity change with total loss of sodium and a Doppler reactivity change with fuel temperature rise about equal to that calculated for the earlier reference design can be achieved with an overall fuel economy about equal to that of the earlier design. That is, the higher breeding ratio and the reduced specific power about balance each other in the design which achieves the above Doppler and sodium-loss reactivity effects. Reducing the large resistance to heat transfer in the fuel-clad gap, item e. above, in combination with item a., permits these Doppler and sodium effects to be realized without appreciable reduction of specific power and, hence, leaves a net improvement in the fuel economics (not taking into account here any increase of fabrication cost in order to improve the fuel heat transfer properties). In this case, some compromise of limits on excess operating reactivity or of the operating interval between refuelings must be made.

Introducing a small amount of moderating material into the core, item c., produced a very large increase of the Doppler effect. For example, 8 v/o BeO increased the Doppler coefficient about 70 per cent. Combining items a., b., and c., appears to offer a good balance between safety and economics considerations, with e. offering a potential improvement. Modifications of core configuration, item d., have not yet been evaluated by actual calculations; but several possibilities are being considered in connection with increasing the reactor size to a 1000 MW(e) plant.

7.1.2 Results on Reference Design

7.1.2.1 Comparison with Earlier Results

A reactor size and composition very nearly that of the 500 MW(e) reference design case [1] was considered. Its dimensions and composition in the hot operating condition are as follows:

Core: 3.3-foot length and 6.6-foot diameter;
32 v/o PuO_2-UO_2 at 9.6 g/cm^3
16 v/o stainless steel (304) at 7.8 g/cm^3
52 v/o sodium at 0.83 g/cm^3 *

Top and Bottom Axial Blankets:	1.25-foot thickness (each) Same as core composition (with low Pu content from blanket breeding)
Radial Blanket:	1.25-foot thickness 66 v/o UO_2 at 9.6 g/cm^3 (with low Pu content from breeding) 11 v/o stainless steel (304) at 7.8 g/cm^3 23 v/o sodium at 0.83 g/cm^3

Table VII-1 lists several fuel cycle and safety parameters which indicate the changes that resulted from updating the cross sections and calculation methods. The most significant changes are (1) the hardening of the spectrum (2) the higher breeding ratios and lower critical mass, (3) the lower Doppler reactivity effects, and (4) the positive reactivity change due to total loss of sodium.

Table VII-2 shows initial and discharged plutonium isotopic concentrations for the current and earlier evaluations of the reference design fuel cycle. Core values are based on a steady-state recycle of the plutonium, using the plutonium discharged from the blanket as makeup. Table VII-3 shows a neutron balance for the current calculation with equilibrium core and blanket isotopic concentrations.

7.1.2.2 Effect of Total Sodium Loss on Doppler Coefficient

Total loss of sodium coolant considerably hardens the spectrum and reduces the coefficient to about one-half of its original value. The fractional loss of Doppler coefficient increases with fuel temperature as shown by the following computed results:

	Isothermal Doppler Coefficient in $\Delta k/°C$	
Average Fuel Temperature	Sodium	No Sodium
27 C	-14.4×10^{-6}	-8.6×10^{-6}
900 C	-5.0×10^{-6}	-2.3×10^{-6}
1127 C	-4.2×10^{-6}	-1.9×10^{-6}

* The 52 v/o sodium corresponds to the earlier reference design if most of the control rod passages are assumed to be filled with sodium during full power operation.

TABLE VII-1

PHYSICS PARAMETERS FOR REFERENCE DESIGN*

	Current Calculation	Earlier Calculation
Critical Mass, Kg Pu (239+241)		
Core	993	1100
Axial Blankets**	103	98
Radial Blanket**	108	98
Total	1204	1296
Core Fuel Isotopic Composition, a/o		
Pu-239	10.6	10.9
Pu-240	5.2	5.6
Pu-241	1.0	1.9
Pu-242	0.5	0.7
U-238	76.9	75.1
F. P. Pairs	5.8	5.8
Breeding Ratios for Pu(239+241)		
Core	0.76	0.66
Axial Blankets	0.29	0.24
Radial Blanket	0.31	0.18
Total	1.36	1.08
Core Conversion Ratio for Pu(239+241)	0.84	0.73
Doppler Coefficient, $\Delta k/^\circ C$		
Isothermal at 900 C	-5.0×10^{-6}	-7.6×10^{-6}
Spatially Weighted at 27 C Average Temperature	-18.9×10^{-6}	---
Spatially Weighted at 900 C Average Temperature	-5.8×10^{-6}	-9.2×10^{-6}
Spatially Weighted at 1127 C Average Temperature	-4.9×10^{-6}	-7.8×10^{-6}
Doppler Δk for Rapid Fuel Temperature Transients***		
Isothermal at 27 C to Peak Just Above Melting Point (2760 C)	-0.0116	-0.0194
Average at 1127 C to Peak at 3600 C	-0.0035	-0.0049
Average at 900 C to Peak at 3600 C	-0.0048	-0.0071

* Values listed are for average fuel isotopic concentrations in a steady state cycle with 100,000 MWD/t irradiations for each fuel batch discharged from the core. Thus the above values correspond to a core which is about at 50,000 MWD/t exposure (the average overall of the fuel batches ranging from 0 to 100,000 MWD/t), and to blanket fuel which, on the average, has been in the reactor for the time required to reach 50, 000 MWD/t core exposure. (MWD/t is thermal megawatt days per 2000 pounds of U+Pu.) Calculated reactivity of this core composition is 1.018.

** Uranium in the blankets is initially at 0.4 per cent enrichment (depleted U). Core uranium is fully depleted.

*** Fuel temperature goes from an initial to a final temperature distribution as indicated. "Isothermal" means all fuel is at the same temperature, "Average" refers to the fuel at average core power density, and "Peak" refers to the center of the hottest fuel pellet in the core.

TABLE VII-1 (Continued)

	Current Calculation	Earlier Calculation
Total Loss of Sodium Reactivity Change, Δk		
Axial Calculations		
Core Only	+ 0.0144	---
Core and Top and Bottom Blankets	+ 0.0063	~ 0.
Radial Calculations		
Core and Blanket	+ 0.0071	---
Operating Reactivity for Burnup at 0.8 Load Factor		
Δk per 4 months at 1000 KW/Kg Pu(239+241)	-0.013	-0.011
$ per 4 months at 1000 KW/Kg Pu(239+241)	-3.6	-3.1
Delayed Neutron Fraction*	0.0042	0.0036
Effective Delayed Neutron Fraction, $\Delta k/\$$	0.0036	---
Mean Neutron Energy of Power Spectrum, Kev*	210	180
Fraction of Fissions by Neutrons Below 9 Kev*	0.133	~0.15
Prompt Neutron Lifetime, 10^{-7} sec	4.4	~5
Power Distributions		
Fraction in Core	0.89	0.86
Fraction in Axial Blankets	0.06	0.08
Fraction in Radial Blanket	0.05	0.06
Core Radial Peak/Average	1.7	1.7
Core Axial Peak/Average	1.2	1.2

* Evaluated in core region of average $\phi\phi^{\dagger}$ (where $\phi^{\dagger}$ is adjoint flux) for current calculation.

TABLE VII-2

INITIAL AND DISCHARGE PLUTONIUM ISOTOPIC CONCENTRATIONS

10^5 MWD/T IN CORE-STEADY STATE RECYCLE

WITH BLANKET PU FOR CORE MAKEUP

	Atom Percent of Listed Isotope in Total (U+Pu+FP Pairs)					
	Pu-239	Pu-240	Pu-241	Pu-242	Pu(239+241)	Total Pu
Current Calculation*						
Core Initial (Clean)	12.0	5.3	1.0	0.5	13.0	18.8
Core Discharge	9.3	5.1	1.0	0.5	10.3	15.9
Axial Blanket Discharge	2.87	0.17	0.01	~ 0	2.88	3.05
Radial Blanket Discharge	1.62	0.05	~ 0	~ 0	1.62	1.67
Earlier Calculation						
Core Initial	12.3	5.1	2.5	0.6	14.8	20.5
Core Discharge	9.6	5.9	1.5	0.8	11.1	17.8
Axial Blanket Discharge	~ 3.0					
Radial Blanket Discharge	~ 1.6					

* Mass of (U+Pu+fission products) in core is 8550 Kg; in axial blankets, 6480 Kg; in radial blanket, 16100 Kg, for radial-blanket height equal to core height only.

TABLE VII-3

NEUTRON BALANCE FOR REFERENCE DESIGN

Material	Core Only		Core Only	
	Percent Fissions	Percent Captures	Percent Fissions	Percent Captures
FP	0	2.61	0	2.71
Oxygen	0	0.15	0	0.19
Sodium	0	0.47	0	0.70
Stainless Steel	0	1.77	0	2.49
U-238	3.84	22.63	5.18	42.38
Pu-239	22.17	5.07	24.06	5.67
Pu-240	1.78	3.43	1.78	3.47
Pu-241	3.11	0.44	3.11	0.44
Pu-242	0.15	0.28	0.15	0.28
U-235	0	0	0.51	0.21
U-236	0	0	0	0.01
Totals	31.05	36.85	34.79	58.55
Leakage		21.68		6.66
Leakage+Captures		58.53		65.21
Leakage+Captures+Fissions		89.58		100.00

7.1.2.3 Dependence of Doppler Effect and Specific Power on Fuel Temperature

The isothermal Doppler coefficient is approximately inversely proportional to the absolute fuel temperature. It is fitted very well to the relationship

$$\left(\frac{dk}{dT}\right)_{Dop} = -\frac{A}{T} + \frac{B}{T^2} \qquad (1)$$

where T is the average fuel temperature in °K, and for the reference case, A = 0.00635 and B = 0.6. The SPARTA code, described in Section 7.3.1, computes a Doppler coefficient corrected for the effects of spatially non-uniform flux and fuel temperature distributions, using space-dependent and temperature-dependent Doppler coefficient data computed by perturbation theory as

input. SPARTA also calculates the Doppler reactivity change for a rapid fuel temperature transient in which the initial fuel temperature distribution T rises to a final distribution T . The final temperature distribution T' takes into account the effect of the heat of fusion for that portion of the fuel which reaches the melting point.

Table VII-4 lists Doppler coefficient and Δk values calculated with the SPARTA code for a range of operating average fuel temperature values. The Δk has been converted to dollar reactivity units, and it is for a transient in which the center of the hottest oxide fuel pellet goes through a phase transition and reaches a temperature of 3600 C in the liquid state. It is seen that the Doppler reactivity available for terminating such a transient rises appreciably as the average fuel temperature at rated power is lowered. This is because (1) the Doppler coefficient increases as temperature is lowered, and (2) a larger fuel temperature rise may be tolerated in the transient when starting from a lower fuel temperature.

Fuel specific power, total reactor power, and excess operating reactivity are also listed in Table VII-4 as functions of the average fuel temperature at rated power. Thermal parameters assumed for the calculations are given in footnotes of the table. The excess operating reactivity values are for a four-month operating period between refuelings and may be raised or lowered in direct proportion to the refueling period.

7.1.3 Modifications of Core Composition to Improve Safety Characteristics

7.1.3.1 Increase of Sodium Volume and Reduction of Fuel Density

A core composition modified to 28 v/o PuO_2-UO_2, 14 v/o steel, and 58 v/o sodium, with the same size and shape as the reference case, gave a zero reactivity change upon total loss of sodium coolant from core and blankets. The Doppler effects were only about 5 per cent less than those of the reference design. However, the required Pu(239+241) enrichment at half burnup was increased from 11.6 to 12.4 a/o. Also the excess operating reactivity for a given refueling period was increased by 30 per cent due to a reduction of the core conversion ratio.

TABLE VII-4

VARIATIONS OF DOPPLER EFFECT, EXCESS OPERATING REACTIVITY, SPECIFIC POWER, AND TOTAL POWER WITH AVERAGE FUEL TEMPERATURE

Avg. Fuel Temp. °C	$\left(\frac{dk}{dT}\right)_{Dop} \times 10^6$	$\left(\frac{(\Delta k)_{\bar{T}\rightarrow\bar{T}'}}{\beta}\right)$ (a) Dollars	Oper. Reactivity $(\Delta k/\beta)$ (b) Dollars	Fuel Specific Power in Core $\left(\frac{kw(t)}{kg\ Pu\ (239+241)}\right)$	Reactor Power (e) MW(e)
800	-6.2	-1.50	-2.1	595 (c)	250
900	-5.8	-1.33	-2.8	785 (c)	330
1000	-5.4	-1.17	-3.5	980 (c)	410
1100	-5.0	-1.02	-4.2	1170 (c)	490
1200	-4.7	-0.89	-4.9	1360 (c)	570
800	-6.3	-1.47	-3.2	865 (d)	360
900	-5.9	-1.30	-4.1	1140 (d)	475
1000	-5.5	-1.14	-5.1	1420 (d)	590
1100	-5.1	-0.99	-6.1	1700 (d)	710
1200	-4.8	-0.86	-7.1	1980 (d)	825

(a) Final average fuel temperature $\bar{T}'$ is calculated to give a peak final fuel temperature (at center of hottest pellet) of 3600 C. Power peaking factors used are listed in Table VII-1. Heat of fusion for oxide is taken as 63 cal/g.

(b) For four months operation between refueling, at 0.8 load factor.

(c) Based on fuel thermal conductivity of 2.0 Btu/hr-ft-°F (≅ .035 watts/cm-°C) and a fuel-clad gap coefficient of 1000 Btu/hr-ft^2-°F (≅ 0.57 watts/cm^2-°C). Fuel diameter (inside clad) is 0.22-inch (=0.56 cm). Clad and clad-coolant surface thermal resistances are neglected. Coolant is at 490 C average.

(d) Gap coefficient increased to 3000 Btu/hr-ft^2-°F.

(e) For a 37 per cent thermal efficiency.

7.1.3.2 Use of Moderating Material in the Core

An approach to increasing the Doppler coefficient involves incorporating a small amount of moderating material into the core to further degrade the fast neutron spectrum. Several materials may be considered for this purpose; among them being BeO, Be, C, MgO, Al_2O_3, and others containing light elements. Nickel, which is not especially light, may also be used in alloy or compound form as a structural or additive material to improve the Doppler coefficient because of its exceptionally high scattering cross section in the resonance region below 10 Kev.

To illustrate this approach, calculations were carried out with 8 v/o BeO as the additive moderating material. Three cases were considered, with BeO replacing sodium in one case and fuel in a second case. The third case is a modification of the second, with an increased sodium volume and a lowered fuel volume to reduce the reactivity increment with total loss of sodium. Results of these calculations are listed in Table VII-5. It is seen that an appreciable increase of Doppler effect results from the small increment of BeO.

7.2 Debye Temperature and Doppler Calculations

The effect of uncertainties in the Debye temperature of UO_2 on Doppler reactivity changes with changes in fuel temperature has been studied. Calculations for UO_2[4] have yielded Debye temperatures ranging from 154 K to 870 K. If the lower end of this range is correct, crystalline binding in the UO_2 lattice has negligible effect on the Doppler coefficient in the temperature range of interest. Debye temperatures in the region of 900 K have only a small effect. For example, a 900 K Debye temperature yields a Doppler reactivity change for a fuel temperature rise from 300 K to 1000 K which is about 20 per cent less in magnitude than that computed neglecting the crystalline binding effects (i. e., zero Debye temperature). This is of interest primarily for interpretation of low temperature Doppler coefficient measurements. For fuel temperatures above the Debye value, crystalling binding produces essentially no effect on the Doppler coefficient. Thus, if the Debye temperature of the mixed PuO_2-UO_2 lattice is not larger than 900 K (believed to be the upper limit of the uncertainty range for UO_2), the calculated Doppler coefficient for the FCR at rated power is not affected by considerations of crystalline binding.

TABLE VII-5

EFFECTS OF ADDING MODERATING MATERIAL

ON FCR PHYSICS PARAMETERS*

	A Reference FCR	B BeO Displaces Sodium	C BeO Displaces Fuel	D More Sodium Than C
Core Composition				
v/o PuO_2-UO_2	32	32	24	22.5
v/o Steel	16	16	16	15
v/o Sodium	52	44	52	55
v/o BeO	0	8	8	7.5
Core Critical Mass, Kg Pu (239+241)	993	993	898	880
a/o Pu(239+241)	11.6	11.6	14.0	14.6
Total Breeding Ratio	1.36	1.33	1.26	1.22
Excess Reactivity for 4 Months Refueling Period at 1000 KW/Kg	0.013	0.013	0.023	0.025
Doppler Δk for Isothermal Temperature Rise from 300 K to 1400 K	-0.0082	-0.015	-0.014	-0.013
Δk for Total Loss of Sodium	+0.0071	**	+0.0025	+0.0004

* See footnotes accompanying Table VII-1 for further explanation of assumed conditions.

** Not calculated for Case B since relative coefficients indicate sodium problem is aggravated with this composition.

7.3 Methods Development

7.3.1 SPARTA Code

A computer code SPARTA, which corrects isothermal Doppler coefficients for spatial temperature and flux distributions in the reactor, has been programmed on the TRANSAC-2000. This program calculates Doppler coefficients and also reactivity changes resulting from rapid fuel temperature transients. In the SPARTA calculation, the core is subdivided into a number of regions as specified by input, and the fuel rod at the average fuel temperature of each region is further subdivided into a specified number of annular zones; and the average temperature of each zone is computed. Input to the code consists of isothermal Doppler coefficient data for the several radial and axial regions into which the core has been subdivided, core power distribution data, the average fuel temperature of the core, the average coolant temperature, the fraction of temperature rise from coolant to fuel-average which occurs between the coolant and the outside of the fuel rod, and the peak fuel temperature at the end of a rapid transient. Fuel temperatures at the end of the transient are corrected for the heat of fusion in the portion of the fuel that reaches the melting point.

7.3.2 Fuel Rod Temperature Distribution in Doppler Calculations

An analysis was made to determine the correction to be applied to the Doppler coefficient to take into account the parabolic temperature distribution across an individual fuel rod. It was found that an effective temperature

$$T_{eff} \approx \bar{T} \left[1 - 1/4 \left(1 - \frac{T_o}{\bar{T}} \right)^2 \right] \qquad (2)$$

is applicable in first order for a rod diameter which is small compared with a neutron mean free path; where $\bar{T}$ is the average fuel temperature and T_o the temperature on the outer radius of the fuel rod (all temperatures in absolute units). In the FCR, T_{eff} differs from $\bar{T}$ by only about two per cent; hence, the Doppler coefficient is increased by only this small amount due to the parabolic temperature distribution across a fuel rod.

The SPARTA code takes into account the parabolic rod temperature distribution by averaging the Doppler coefficient over the temperature distribution. This is valid only when the rod diameter is large compared with the neutron mean free path -- a condition that is not satisfied in the

FCR or any other fast reactor. It was determined, however, that in first order this approach is equivalent in FCR to using an effective temperature

$$T_{eff} = \bar{T} \left[1 - 1/3 \left(1 - \frac{T_o}{\bar{T}} \right)^2 \right] \quad (3)$$

which is in good agreement with equation (2) considering that the correction term is extremely small.

Calculations on the FCR reference design with the SPARTA code show that the spatial distribution of fuel temperature and of neutron flux and importance increases the isothermal Doppler coefficient corresponding to the average fuel temperature by 17 per cent. About 15 per cent of this increment is due to the gross spatial distributions across the entire core, and only two per cent is due to the temperature distribution across the individual fuel rods.

7.3.3 Report on Doppler Calculation Methods

A draft of the report on Doppler calculation methods has been completed, and will be issued as GEAP-4092 after review and approvals have been obtained. More detailed descriptions of items 7.2, 7.3.1, and 7.3.2 above, are included in this report.

7.3.4 FORE Code

A report describing the FORE computer code for analysis of fast reactor excursions has been completed (GEAP-4090) and a report on the results of calculations using the FORE code is being written. This report will cover the effects of

a. Total reactivity insertion and rate of insertion.

b. Individual feedback mechanisms in various combinations. including Doppler effect and clad, coolant, and fuel density changes.

c. Initial conditions (power, coolant flow, and coolant temperature).

d. Variations in neutron lifetime, fuel conductivity and fuel-clad heat transfer coefficient, Doppler coefficient, and fuel heat of fusion.

e. Step changes in coolant flow and temperature.

7.3.5 FARM Code

The FARM code for analysis of fast reactor meltdown accidents has been debugged, and a first draft of a report describing the code has been written. Efficient use of the code, however, will require the accumulation of much additional operating experience.

7.4 References

1. GEAP-3721, "Core Design Study for a 500 MW(e) Fast Oxide Reactor". K. M. Horst, B. A. Hutchins, F. J. Leitz, and B. Wolfe; December 28, 1961.
2. GEAP-3646, "Calculation of Doppler Coefficient and Other Safety Parameters for a Large Fast Oxide Reactor". P. Greebler, B. A. Hutchins, J. R. Sueoka; March 9, 1961.
3. "The Doppler Effect in a Large Fast Oxide Reactor - Its Calculation and Significance for Reactor Safety". P. Greebler and B. A. Hutchins; Seminar on the Physics of Fast and Intermediate Reactors; Vienna, Austria; August 3 -11, 1961.
4. J. Belle, Editor, Uranium Dioxide, United States Atomic Energy Commission, (1961).